

## DC to 28 GHz, GaAs, pHEMT, 2 W Power Amplifier

### FEATURES

- ▶ Wideband, internally-matched, RF power amplifier
- ▶ DC-coupled input and output
- ▶ Integrated RF power detector
- ▶ Integrated temperature sensor
- ▶ Gain: 12.5 dB typical at 2 GHz to 16 GHz
- ▶ OP1dB: 33 dBm typical at 2 GHz to 16 GHz
- ▶ P<sub>SAT</sub>: 34 dBm typical at 2 GHz to 16 GHz
- ▶ OIP3: 45 dBm typical at 2 GHz to 16 GHz
- ▶ 32-Lead, 5.00 mm × 5.00 mm, LFCSP\_CAV package

### APPLICATIONS

- ▶ Electronic warfare
- ▶ Radar
- ▶ Test and measurement equipment

### GENERAL DESCRIPTION

The ADPA9007 is a 2 W, RF power amplifier that operates from DC to 28 GHz. The RF input and output are internally-matched and DC-coupled. The ADPA9007 includes an integrated temperature-compensated RF power detector and an integrated temperature sensor.

The ADPA9007 amplifier provides a gain of 12.5 dB, an output power for 1 dB compression (OP1dB) of 33 dBm, and an output third-order intercept (OIP3) of 45 dBm from 2 GHz to 16 GHz. The amplifier operates from a typical supply voltage of 15 V and has a 500 mA typical quiescent bias current, which is adjustable.

The ADPA9007 is fabricated on a gallium arsenide (GaAs), pseudomorphic high electron mobility transistor (pHEMT) process. The amplifier is housed in an RoHS-compliant, 32-Lead, 5 mm × 5 mm, lead frame chip scale package, premolded cavity [LFCSP\_CAV] and is specified for operation from -40°C to +85°C.

### FUNCTIONAL BLOCK DIAGRAM

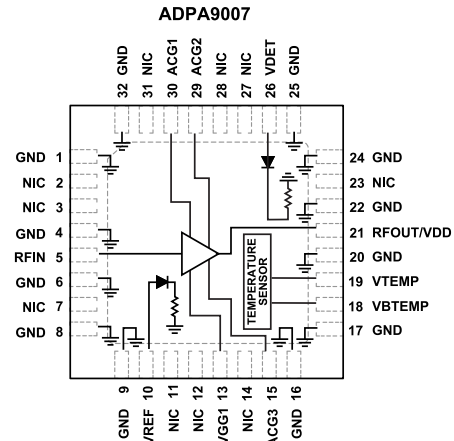


Figure 1. Functional Block Diagram

001

**TABLE OF CONTENTS**

Features.....	1	Interface Schematics.....	8
Applications.....	1	Typical Performance Characteristics.....	9
General Description.....	1	Theory of Operation.....	22
Functional Block Diagram.....	1	Applications Information.....	23
Specifications.....	3	Power-Up Sequencing.....	23
0.05 GHz to 2 GHz Frequency Range.....	3	Power-Down Sequencing.....	23
2 GHz to 16 GHz Frequency Range.....	3	Biasing the ADPA9007 with the HMC980LP4E...	24
16 GHz to 20 GHz Frequency Range.....	4	Application Circuit Setup.....	24
20 GHz to 24 GHz Frequency Range .....	4	Limiting VGATE for the ADPA9007 $V_{GG1}$ .....	24
24 GHz to 28 GHz Frequency Range.....	5	HMC980LP4E Bias Sequence.....	25
Absolute Maximum Ratings.....	6	Constant Drain Current Biasing vs.	
Thermal Resistance.....	6	Constant Gate Voltage Biasing.....	25
Electrostatic Discharge (ESD) Ratings .....	6	Outline Dimensions.....	28
ESD Caution.....	6	Ordering Guide.....	28
Pin Configuration and Function Descriptions.....	7	Evaluation Boards.....	28

**REVISION HISTORY****12/2023—Revision 0: Initial Version**

## SPECIFICATIONS

## 0.05 GHZ TO 2 GHZ FREQUENCY RANGE

$T_{CASE} = 25^{\circ}C$ , supply voltage ( $V_{DD}$ ) = 15 V, and quiescent drain current ( $I_{DQ}$ ) = 500 mA, unless otherwise noted. Adjust the gate voltage ( $V_{GG1}$ ) from -1.5 V to 0 V to achieve  $I_{DQ} = 500$  mA typical.

Table 1. 0.05 GHz to 2 GHz Frequency Range

Parameter	Test Conditions/Comments	Min	Typ	Max	Unit
FREQUENCY RANGE		0.05		2	GHz
GAIN		11	13		dB
Flatness			±1.05		dB
Variation over Temperature			0.02		dB/°C
NOISE FIGURE			10		dB
RETURN LOSS					
Input			14		dB
Output			15		dB
OUTPUT					
OP1dB		29	31		dBm
Saturated Output Power ( $P_{SAT}$ )			34		dBm
OIP3	Output power ( $P_{OUT}$ ) per tone = 16 dBm with 1 MHz tone spacing		43		dBm
OIP2	$P_{OUT}$ per tone = 16 dBm with 1 MHz tone spacing		48		dBm
SUPPLY					
$I_{DQ}$	Adjust $V_{GG1}$ to achieve $I_{DQ} = 500$ mA typical		500		mA
$V_{DD}$		10		15	V

## 2 GHZ TO 16 GHZ FREQUENCY RANGE

$T_{CASE} = 25^{\circ}C$ ,  $V_{DD} = 15$  V, and  $I_{DQ} = 500$  mA, unless otherwise noted. Adjust  $V_{GG1}$  from -1.5 V to 0 V to achieve  $I_{DQ} = 500$  mA typical.

Table 2. 2 GHz to 16 GHz Frequency Range

Parameter	Test Conditions/Comments	Min	Typ	Max	Unit
FREQUENCY RANGE		2		16	GHz
GAIN		10.5	12.5		dB
Flatness			±0.26		dB
Variation over Temperature			0.016		dB/°C
NOISE FIGURE			4		dB
RETURN LOSS					
Input			13		dB
Output			15		dB
OUTPUT					
OP1dB		31	33		dBm
$P_{SAT}$			34		dBm
OIP3	$P_{OUT}$ per tone = 16 dBm with 1 MHz tone spacing		45		dBm
OIP2	$P_{OUT}$ per tone = 16 dBm with 1 MHz tone spacing		45		dBm
SUPPLY					
$I_{DQ}$	Adjust $V_{GG1}$ to achieve $I_{DQ} = 500$ mA typical		500		mA
$V_{DD}$		10		15	V

## SPECIFICATIONS

## 16 GHZ TO 20 GHZ FREQUENCY RANGE

$T_{CASE} = 25^{\circ}C$ ,  $V_{DD} = 15 V$ , and  $I_{DQ} = 500 mA$ , unless otherwise noted. Adjust  $V_{GG1}$  from  $-1.5 V$  to  $0 V$  to achieve  $I_{DQ} = 500 mA$  typical.

Table 3. 16 GHz to 20 GHz Frequency Range

Parameter	Test Conditions/Comments	Min	Typ	Max	Unit
FREQUENCY RANGE		16		20	GHz
GAIN		10.5	12.5		dB
Flatness			$\pm 0.1$		dB
Variation over Temperature			0.002		dB/ $^{\circ}C$
NOISE FIGURE			3.5		dB
RETURN LOSS					
Input			14		dB
Output			17		dB
OUTPUT					
OP1dB		29	31		dBm
$P_{SAT}$			33.5		dBm
OIP3	$P_{OUT}$ per tone = 16 dBm with 1 MHz tone spacing		43		dBm
OIP2	$P_{OUT}$ per tone = 16 dBm with 1 MHz tone spacing		45		dBm
SUPPLY					
$I_{DQ}$	Adjust $V_{GG1}$ to achieve $I_{DQ} = 500 mA$ typical		500		mA
$V_{DD}$		10		15	V

## 20 GHZ TO 24 GHZ FREQUENCY RANGE

$T_{CASE} = 25^{\circ}C$ ,  $V_{DD} = 15 V$ , and  $I_{DQ} = 500 mA$ , unless otherwise noted. Adjust the  $V_{GG1}$  from  $-1.5 V$  to  $0 V$  to achieve  $I_{DQ} = 500 mA$  typical

Table 4. 20 GHz to 24 GHz Frequency Range

Parameter	Test Conditions/Comments	Min	Typ	Max	Unit
FREQUENCY RANGE		20		24	GHz
GAIN			12.5		dB
Flatness					dB
Variation over Temperature			0.008		dB/ $^{\circ}C$
NOISE FIGURE			4		dB
RETURN LOSS					
Input			12		dB
Output			13		dB
OUTPUT					
OP1dB			29		dBm
$P_{SAT}$			32		dBm
OIP3	$P_{OUT}$ per tone = 16 dBm with 1 MHz spacing		43		dBm
SUPPLY					
$I_{DQ}$	Adjust $V_{GG1}$ to achieve $I_{DQ} = 500 mA$ typical		500		mA
$V_{DD}$		10		15	V

## SPECIFICATIONS

## 24 GHz TO 28 GHz FREQUENCY RANGE

$T_{CASE} = 25^{\circ}\text{C}$ ,  $V_{DD} = 15\text{ V}$ , and  $I_{DQ} = 500\text{ mA}$ , unless otherwise noted. Adjust the  $V_{GG1}$  from  $-1.5\text{ V}$  to  $0\text{ V}$  to achieve  $I_{DQ} = 500\text{ mA}$  typical.

Table 5. 24 GHz to 28 GHz Frequency Range

Parameter	Test Conditions/Comments	Min	Typ	Max	Unit
FREQUENCY RANGE		24		28	GHz
GAIN			12		dB
Flatness			$\pm 1.05$		dB
Variation over Temperature			0.017		
NOISE FIGURE			4.5		dB
RETURN LOSS					
Input			13		dB
Output			14		dB
OUTPUT					
OP1dB			27		dBm
$P_{SAT}$			31		dBm
OIP3	$P_{OUT}$ per tone = 16 dBm with 1 MHz tone spacing		39		dBm
SUPPLY					
$I_{DQ}$	Adjust $V_{GG1}$ to achieve $I_{DQ} = 500\text{ mA}$ typical		500		mA
$V_{DD}$		10		15	V

## ABSOLUTE MAXIMUM RATINGS

Table 6. Absolute Maximum Ratings

Parameter	Rating
$V_{DD}$	16.0 V
$V_{GG1}$	-2.0 V to 0 V
RF Input Power (RFIN)	29 dBm
Continuous Power Dissipation ( $P_{DISS}$ ), $T_{CASE} = 85^{\circ}\text{C}$ (Derate 135 mW/ $^{\circ}\text{C}$ above 85 $^{\circ}\text{C}$ )	12.2 W
Temperature	
Maximum Channel	175 $^{\circ}\text{C}$
Quiescent Channel ( $T_{CASE} = 85^{\circ}\text{C}$ , $V_{DD} = 15\text{ V}$ ), $I_{DQ}$ = 500 mA, and Input Power ( $P_{IN}$ ) = Off	140.5 $^{\circ}\text{C}$
Storage Range	-65 $^{\circ}\text{C}$ to +150 $^{\circ}\text{C}$
Operating Range	-40 $^{\circ}\text{C}$ to +85 $^{\circ}\text{C}$

Stresses at or above those listed under Absolute Maximum Ratings may cause permanent damage to the product. This is a stress rating only; functional operation of the product at these or any other conditions above those indicated in the operational section of this specification is not implied. Operation beyond the maximum operating conditions for extended periods may affect product reliability.

## THERMAL RESISTANCE

Thermal performance is directly linked to printed circuit board (PCB) design and operating environment. Careful attention to PCB thermal design is required.

$\theta_{JC}$  is the junction-to-case thermal resistance (channel to exposed metal ground pad on the underside of the device).

Table 7. Thermal Resistance

Package Type	$\theta_{JC}$ <sup>1</sup>	Unit
CG-32-2	7.4	$^{\circ}\text{C}/\text{W}$

<sup>1</sup>  $\theta_{JC}$  was determined by simulation under the following conditions: the heat transfer is due solely to thermal conduction from the channel through the ground pad to the PCB. The ground pad is held constant at 85 $^{\circ}\text{C}$  operating temperature.

## ELECTROSTATIC DISCHARGE (ESD) RATINGS

The following ESD information is provided for handling of ESD-sensitive devices in an ESD-protected area only.

Human Body Model (HBM) per ANSI/ESDA/JEDEC JS-001.

### ESD Ratings for ADPA9007

Table 8. ADPA9007, 32-Lead LFCSP\_CAV

ESD Model	Withstand Threshold (V)	Class
HBM	$\pm 250$	1A

### ESD CAUTION



**ESD (electrostatic discharge) sensitive device.** Charged devices and circuit boards can discharge without detection. Although this product features patented or proprietary protection circuitry, damage may occur on devices subjected to high energy ESD. Therefore, proper ESD precautions should be taken to avoid performance degradation or loss of functionality.

PIN CONFIGURATION AND FUNCTION DESCRIPTIONS

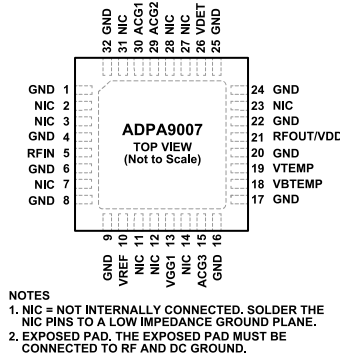


Figure 2. Pin Configuration

Table 9. Pin Function Descriptions

Pin No.	Mnemonic	Description
1, 4, 6, 8, 9, 16, 17, 20, 22, 24, 25, 32	GND	Ground. The GND pins must be connected to the RF and the DC ground. See <a href="#">Figure 3</a> for the interface schematic.
2, 3, 7, 11, 12, 14, 23, 27, 28, 31	NIC	Not Internally Connected. The NIC pins are not connected internally. However, all data shown is measured with the NIC pins connected to RF and DC ground externally.
5	RFIN	RF Input of the Amplifier. The RFIN pin is DC-coupled and matched to 50 Ω. See <a href="#">Figure 4</a> for the interface schematic.
10	VREF	Reference Diode Voltage for the Temperature Compensation of the VDET RF Output Power Measurements. The VREF pin voltage ( $V_{REF}$ ) requires the application of a DC bias voltage through an external series resistor. See <a href="#">Figure 5</a> for the interface schematic.
13	VGG1	Gate Control for the Amplifier. Attach bypass capacitors per the <a href="#">Applications Information</a> section. See the <a href="#">Power-Up Sequence</a> and <a href="#">Power-Down Sequence</a> for additional information. See <a href="#">Figure 6</a> for the interface schematic.
15	ACG3	Low Frequency Termination. Attach bypass capacitors per the <a href="#">Applications Information</a> section. See <a href="#">Figure 4</a> for the interface schematic.
18	VBTEMP	Temperature Sensor Bias. Bias pin for biasing the integrated temperature sensor. See <a href="#">Figure 7</a> for the interface schematic.
19	VTEMP	Integrated Temperature Sensor output. See <a href="#">Figure 7</a> for the interface schematic.
21	RFOUT/VDD	RF Output of the Amplifier. Connect the RFOUT/VDD pin to the DC bias ( $V_{DD}$ ) network to provide drain current ( $I_{DD}$ ). See <a href="#">Applications Information</a> section. See <a href="#">Figure 8</a> for the interface schematic.
26	VDET	Detector Diode Voltage to Measure the RF Output Power. Detection by the VDET pin requires the application of a DC bias voltage through an external series resistor. Used in combination with the VREF pin, the difference detector voltage ( $V_{REF} - V_{DET}$ ) is a temperature compensated DC voltage proportional to the RF output power. See <a href="#">Figure 8</a> for the interface schematic.
29	ACG2	Low Frequency Termination. Attach bypass capacitors per the <a href="#">Applications Information</a> section. See <a href="#">Figure 8</a> for the interface schematic.
30	ACG1	Low Frequency Termination. Attach bypass capacitor per the <a href="#">Applications Information</a> section. See <a href="#">Figure 8</a> for the interface schematic.
	EPAD	Exposed Pad. The exposed pad must be connected to the RF and the DC ground.

PIN CONFIGURATION AND FUNCTION DESCRIPTIONS

INTERFACE SCHEMATICS



Figure 3. GND Interface Schematic

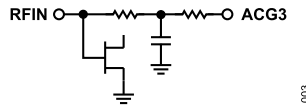


Figure 4. RFIN and ACG3 Interface Schematic

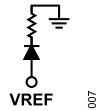


Figure 5. VREF Interface Schematic

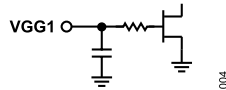


Figure 6. VGG1 Interface Schematic

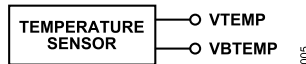


Figure 7. VTEMP and VBTEMP Interface Schematic

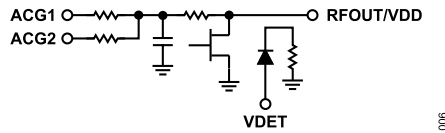


Figure 8. ACG1, ACG2, RFOUT/VDD, and VDET Interface Schematic

TYPICAL PERFORMANCE CHARACTERISTICS

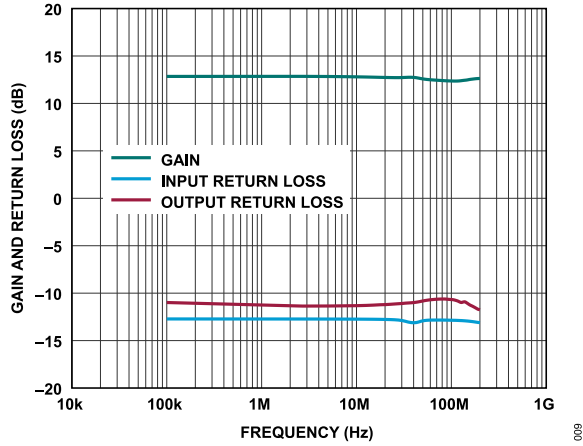


Figure 9. Gain and Return Loss vs. Frequency, 100 kHz to 200 MHz,  $V_{DD} = 15\text{ V}$ ,  $I_{DQ} = 500\text{ mA}$

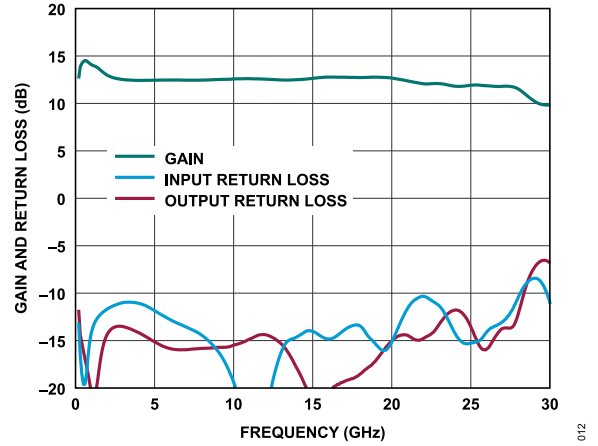


Figure 12. Gain and Return Loss vs. Frequency, 200 MHz to 30 GHz,  $V_{DD} = 15\text{ V}$ ,  $I_{DQ} = 500\text{ mA}$

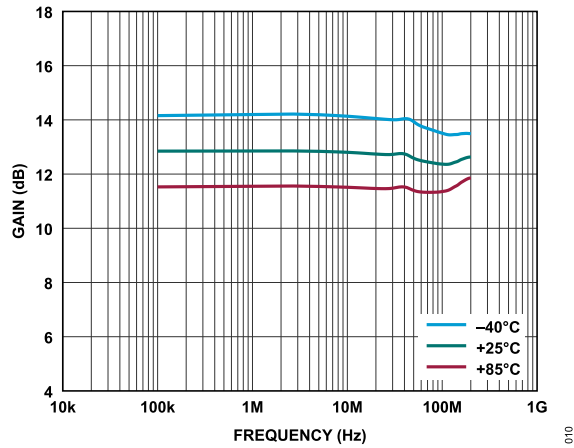


Figure 10. Gain vs. Frequency for Various Temperatures, 100 kHz to 200 MHz,  $V_{DD} = 15\text{ V}$ ,  $I_{DQ} = 500\text{ mA}$

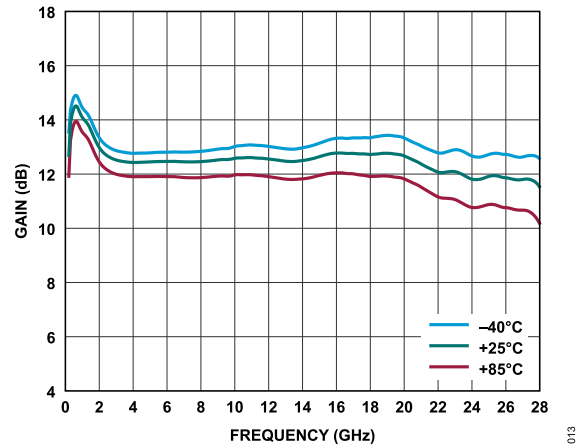


Figure 13. Gain vs. Frequency for Various Temperatures, 200 MHz to 28 GHz,  $V_{DD} = 15\text{ V}$ ,  $I_{DQ} = 500\text{ mA}$

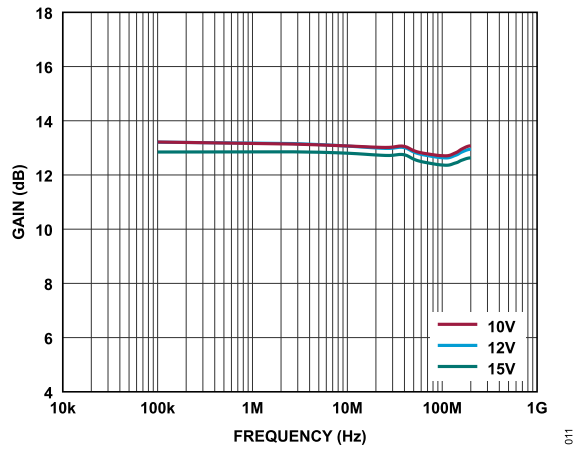


Figure 11. Gain vs. Frequency for Various  $V_{DD}$  Values, 100 kHz to 200 MHz,  $I_{DQ} = 500\text{ mA}$

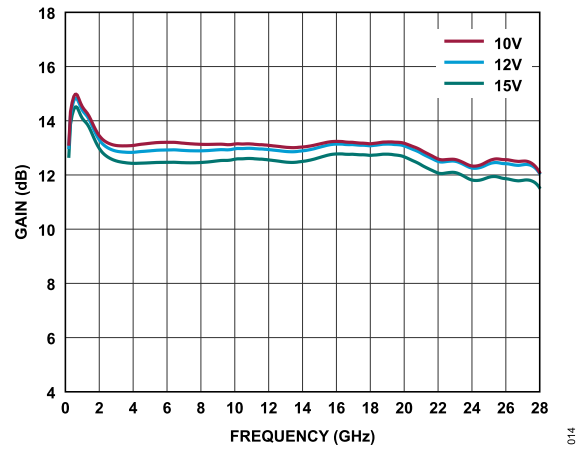


Figure 14. Gain vs. Frequency for Various  $V_{DD}$  Values, 200 MHz to 28 GHz,  $I_{DQ} = 500\text{ mA}$

TYPICAL PERFORMANCE CHARACTERISTICS

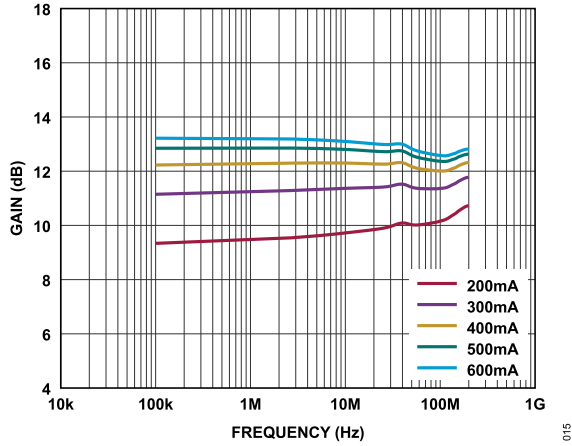


Figure 15. Gain vs. Frequency for Various  $I_{DQ}$  Values, 100 kHz to 200 MHz,  $V_{DD} = 15\text{ V}$

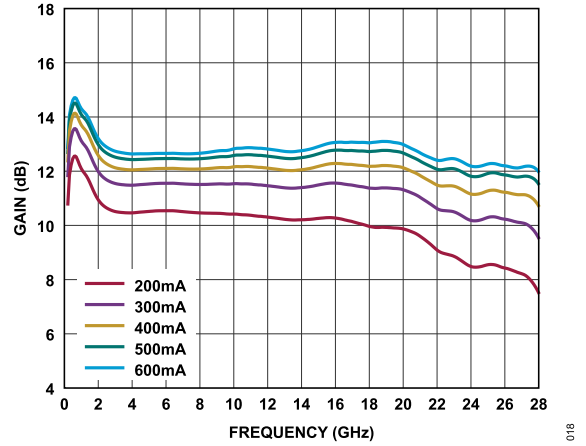


Figure 18. Gain vs. Frequency for Various  $I_{DQ}$  Values, 200 MHz to 28 GHz,  $V_{DD} = 15\text{ V}$

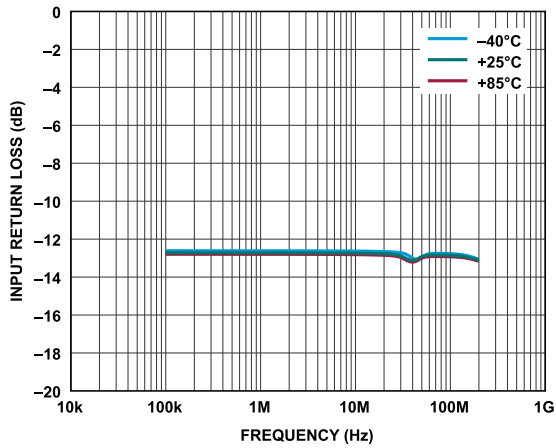


Figure 16. Input Return Loss vs. Frequency for Various Temperatures, 100 kHz to 200 MHz,  $V_{DD} = 15\text{ V}$ ,  $I_{DQ} = 500\text{ mA}$

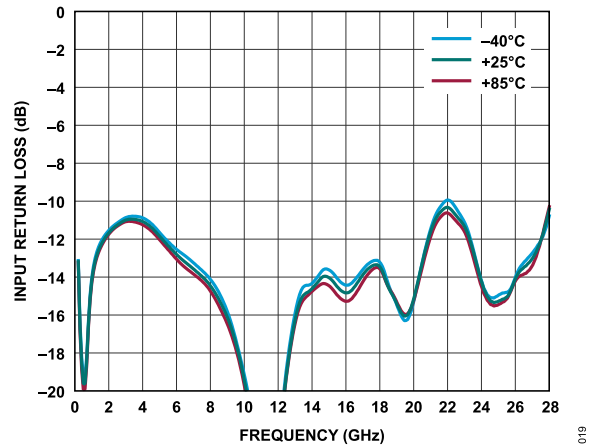


Figure 19. Input Return Loss vs. Frequency for Various Temperatures, 200 MHz to 28 GHz,  $V_{DD} = 15\text{ V}$ ,  $I_{DQ} = 500\text{ mA}$

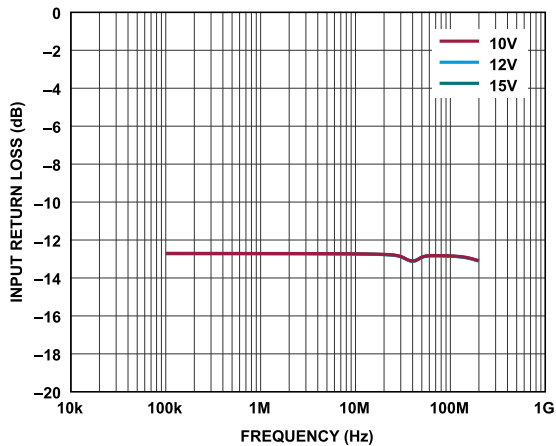


Figure 17. Input Return Loss vs. Frequency for Various  $V_{DD}$  Values, 100 kHz to 200 MHz,  $I_{DQ} = 500\text{ mA}$

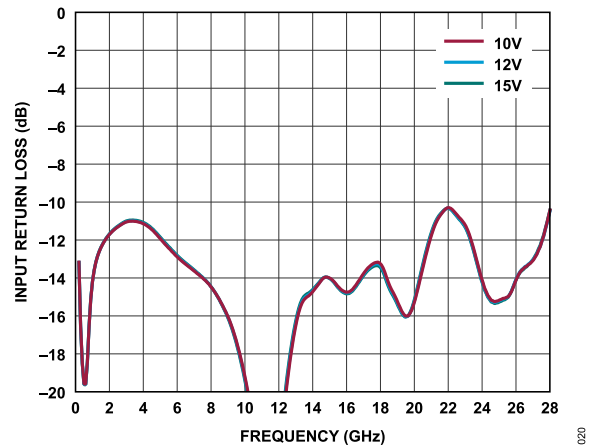


Figure 20. Input Return Loss vs. Frequency for Various  $V_{DD}$  Values, 200 MHz to 28 GHz,  $I_{DQ} = 500\text{ mA}$

TYPICAL PERFORMANCE CHARACTERISTICS

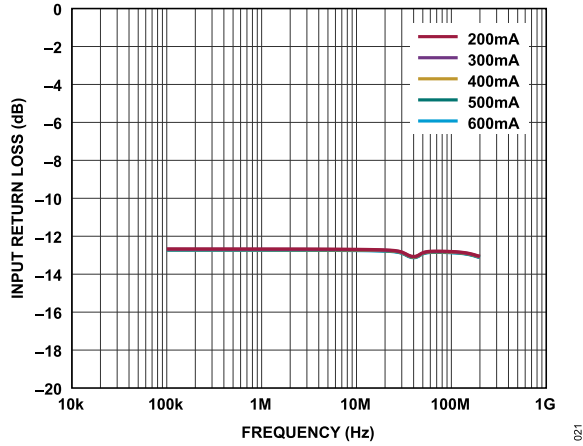


Figure 21. Input Return Loss vs. Frequency for Various  $I_{DQ}$  Values, 100 kHz to 200 MHz,  $V_{DD} = 15 V$

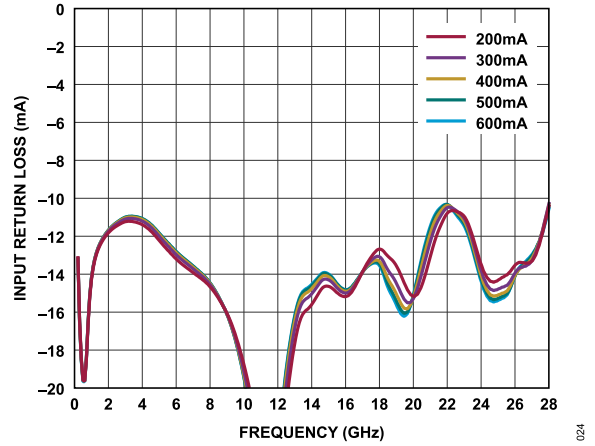


Figure 24. Input Return Loss vs. Frequency for Various  $I_{DQ}$  Values, 200 MHz to 28 GHz,  $V_{DD} = 15 V$

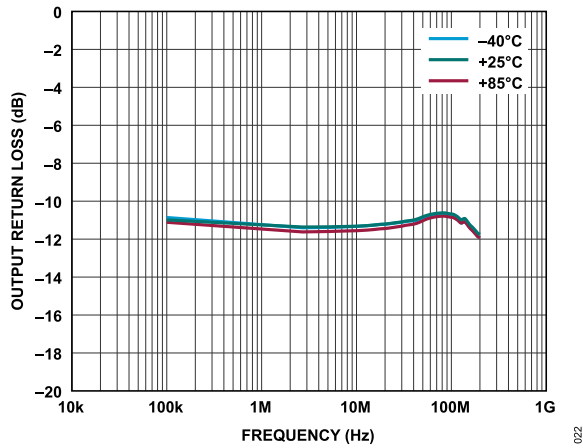


Figure 22. Output Return Loss vs. Frequency for Various Temperatures, 100 kHz to 200 MHz,  $V_{DD} = 15 V$ ,  $I_{DQ} = 500 mA$

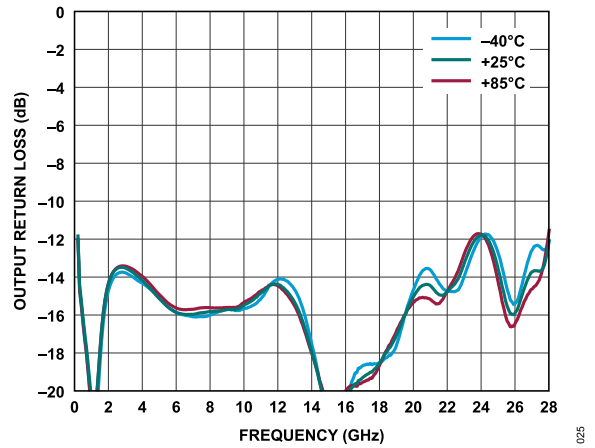


Figure 25. Output Return Loss vs. Frequency for Various Temperatures, 200 MHz to 28 GHz,  $V_{DD} = 15 V$ ,  $I_{DQ} = 500 mA$

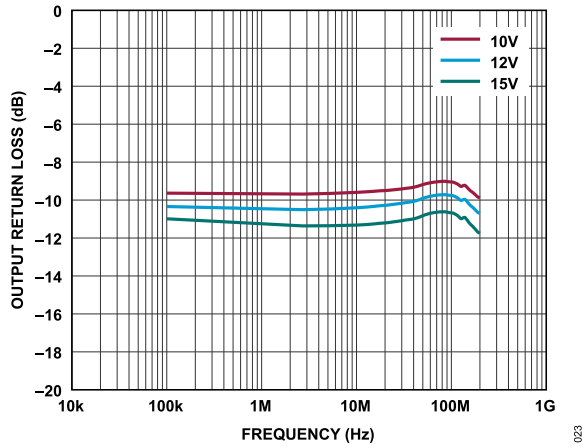


Figure 23. Output Return Loss vs. Frequency for Various  $V_{DD}$  Values, 100 kHz to 200 MHz,  $I_{DQ} = 500 mA$

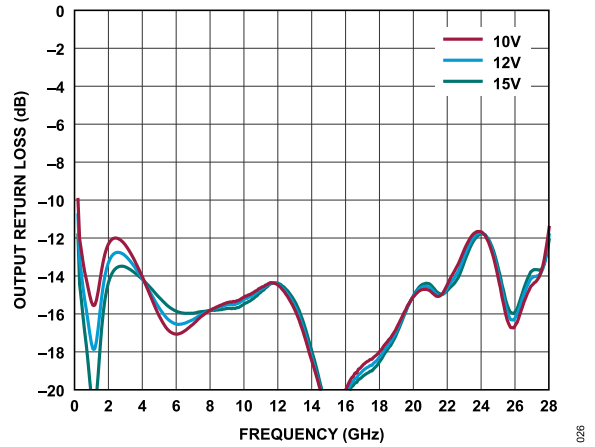


Figure 26. Output Return Loss vs. Frequency for Various  $V_{DD}$  Values, 200 MHz to 28 GHz,  $I_{DQ} = 500 mA$

TYPICAL PERFORMANCE CHARACTERISTICS

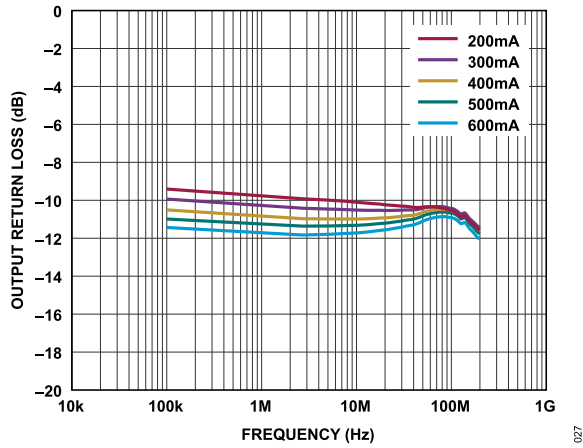


Figure 27. Output Return Loss vs. Frequency for Various  $I_{DQ}$  Values, 100 kHz to 200 MHz,  $V_{DD} = 15 V$

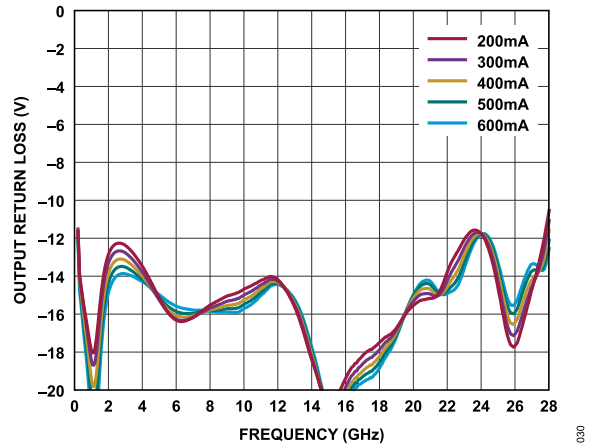


Figure 30. Output Return Loss vs. Frequency for Various  $I_{DQ}$  Values, 200 MHz to 28 GHz,  $V_{DD} = 15 V$

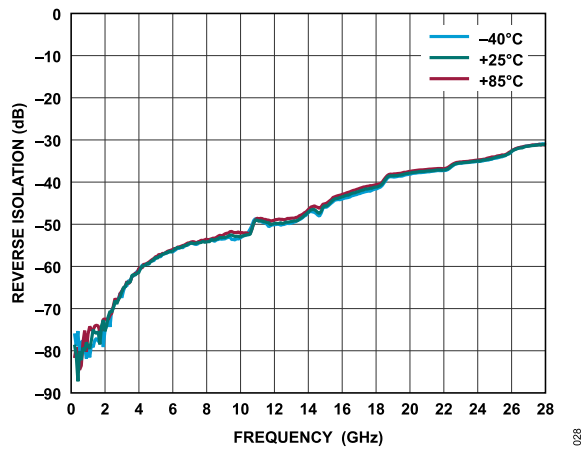


Figure 28. Reverse Isolation vs. Frequency for Various Temperatures,  $V_{DD} = 15 V$ ,  $I_{DQ} = 500 mA$

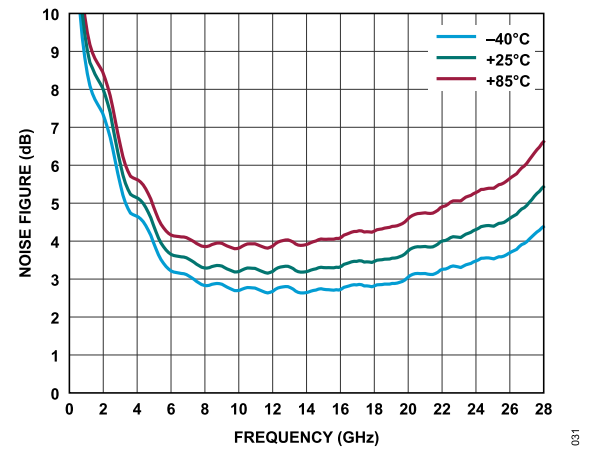


Figure 31. Noise Figure vs. Frequency for Various Temperatures,  $V_{DD} = 15 V$ ,  $I_{DQ} = 500 mA$

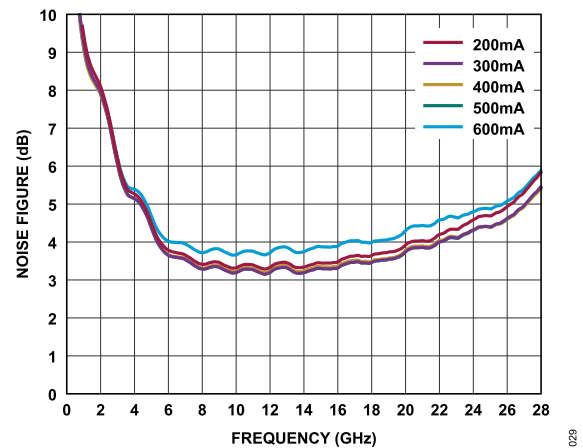


Figure 29. Noise Figure vs. Frequency for Various  $I_{DQ}$  Values,  $V_{DD} = 15 V$

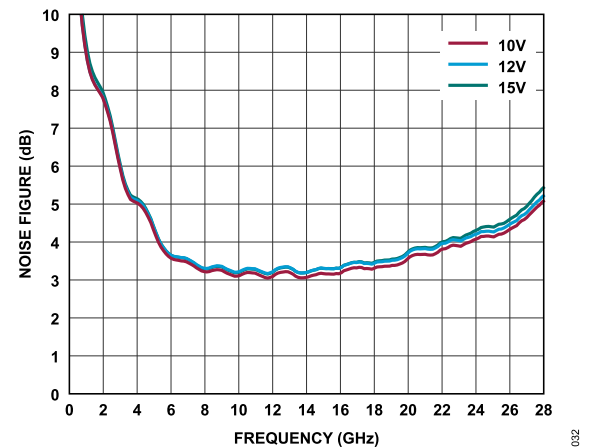


Figure 32. Noise Figure vs. Frequency for Various  $V_{DD}$  Values,  $I_{DQ} = 500 mA$

TYPICAL PERFORMANCE CHARACTERISTICS

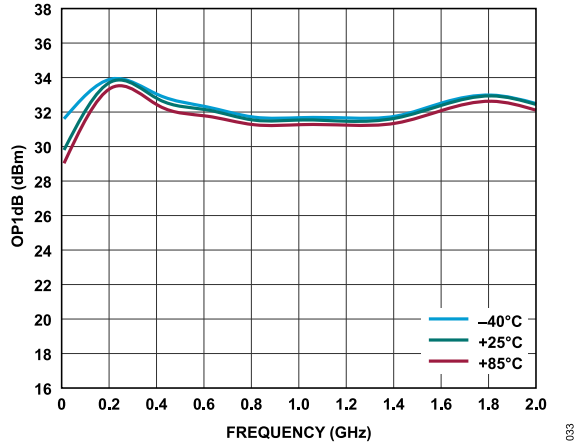


Figure 33. OP1dB vs. Frequency for Various Temperatures, 10 MHz to 2 GHz,  $V_{DD} = 15\text{ V}$ ,  $I_{DQ} = 500\text{ mA}$

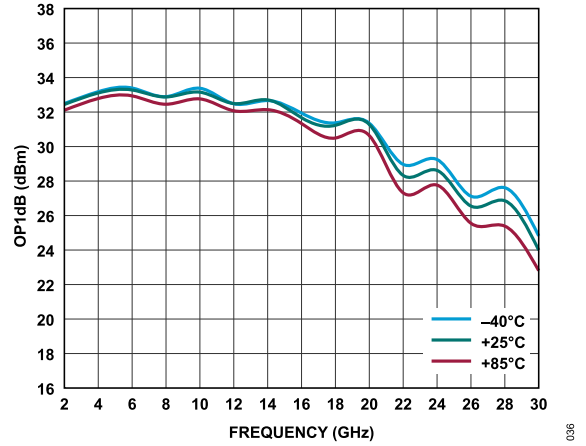


Figure 36. OP1dB vs. Frequency for Various Temperatures, 2 GHz to 28 GHz,  $V_{DD} = 15\text{ V}$ ,  $I_{DQ} = 500\text{ mA}$

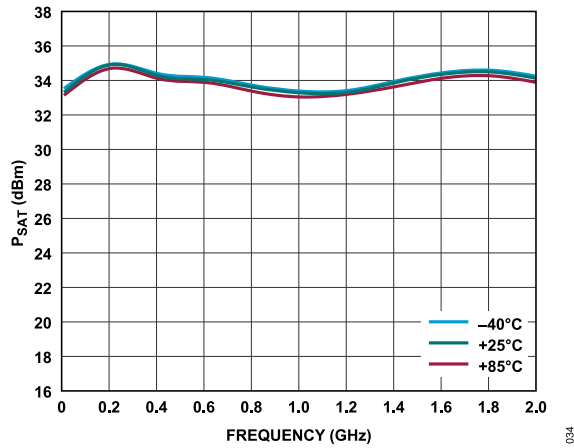


Figure 34.  $P_{SAT}$  vs. Frequency for Various Temperatures, 10 MHz to 2 GHz,  $V_{DD} = 15\text{ V}$ ,  $I_{DQ} = 500\text{ mA}$

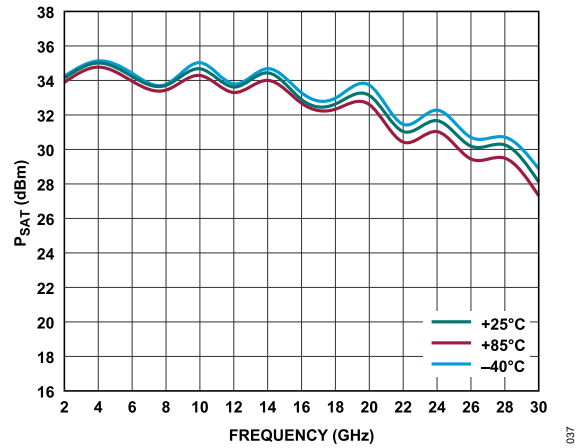


Figure 37.  $P_{SAT}$  vs. Frequency for Various Temperatures, 2 GHz to 28 GHz,  $V_{DD} = 15\text{ V}$ ,  $I_{DQ} = 500\text{ mA}$

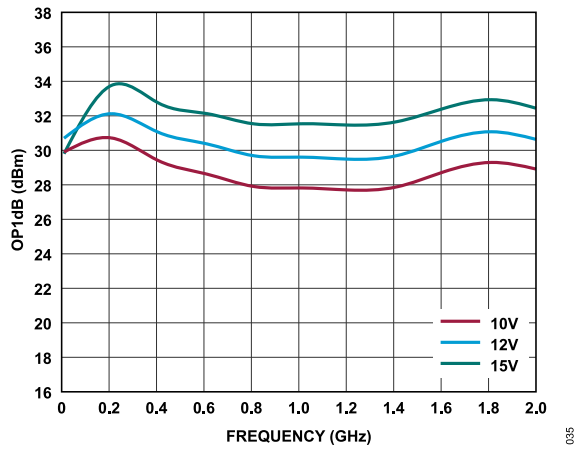


Figure 35. OP1dB vs. Frequency for Various  $V_{DD}$  Values, 10 MHz to 2 GHz,  $I_{DQ} = 500\text{ mA}$

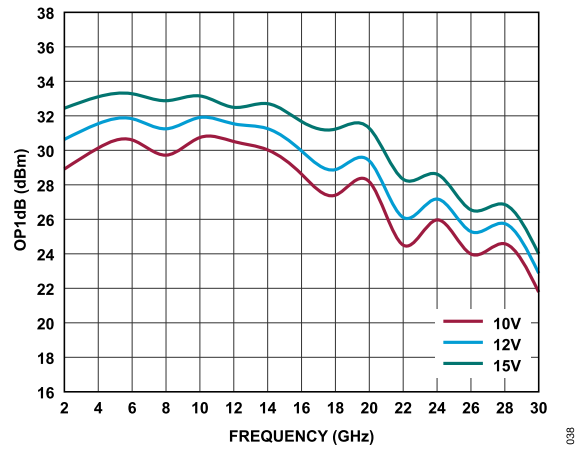


Figure 38. OP1dB vs. Frequency for Various  $V_{DD}$  Values, 2 GHz to 28 GHz,  $I_{DQ} = 500\text{ mA}$

TYPICAL PERFORMANCE CHARACTERISTICS

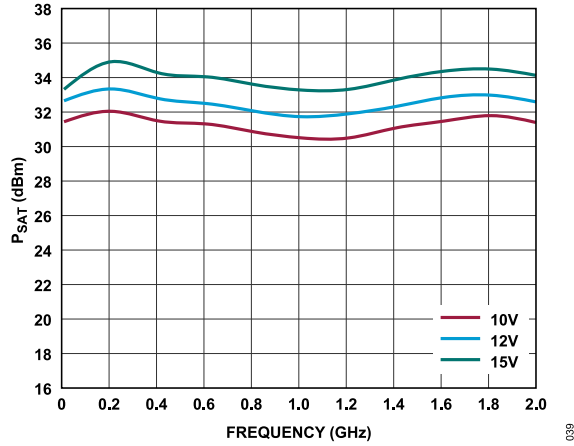


Figure 39.  $P_{SAT}$  vs. Frequency for Various  $V_{DD}$  Values, 10 MHz to 2 GHz,  $I_{DQ} = 500\text{ mA}$

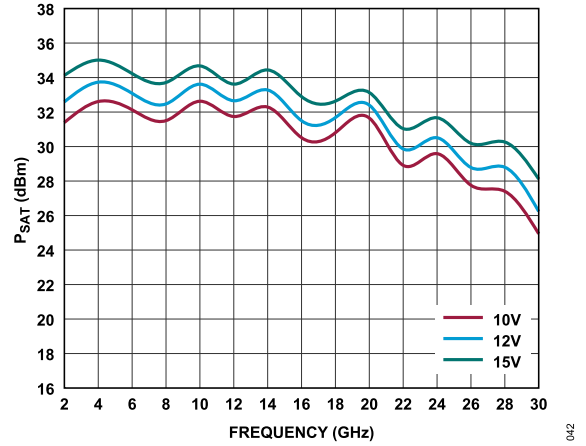


Figure 42.  $P_{SAT}$  vs. Frequency for Various  $V_{DD}$  Values, 2 GHz to 28 GHz,  $I_{DQ} = 500\text{ mA}$

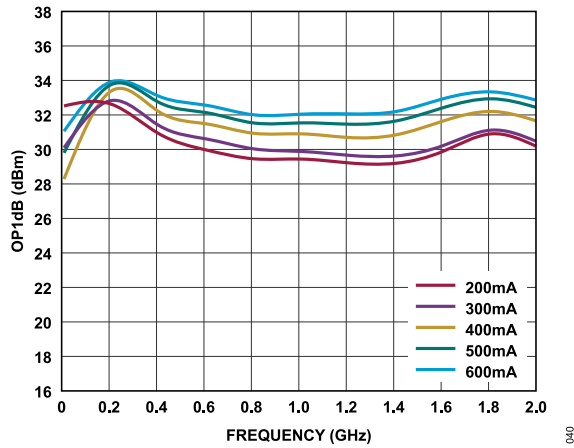


Figure 40.  $OP1dB$  vs. Frequency for Various  $I_{DQ}$  Values, 10 MHz to 2 GHz,  $V_{DD} = 15\text{ V}$

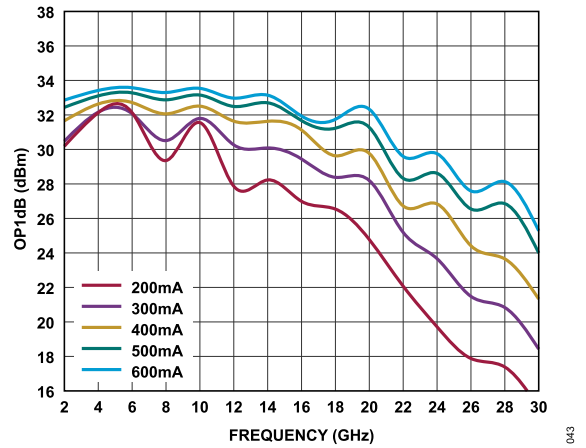


Figure 43.  $OP1dB$  vs. Frequency for Various  $I_{DQ}$  Values, 2 GHz to 28 GHz,  $V_{DD} = 15\text{ V}$

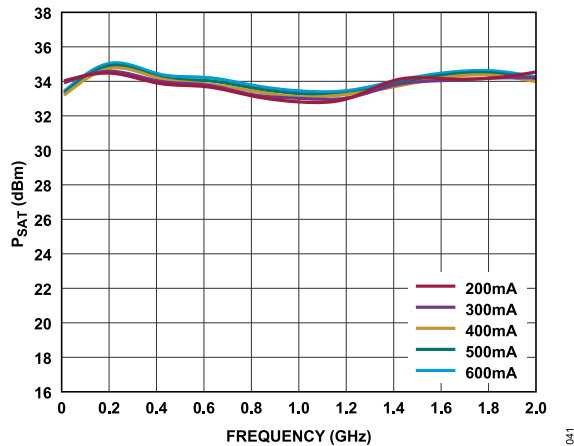


Figure 41.  $P_{SAT}$  vs. Frequency for Various  $I_{DQ}$  Values, 10 MHz to 2 GHz,  $V_{DD} = 15\text{ V}$

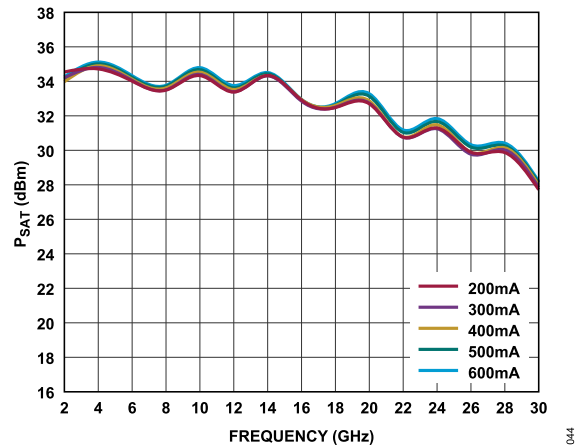


Figure 44.  $P_{SAT}$  vs. Frequency for Various  $I_{DQ}$  Values, 2 GHz to 28 GHz,  $V_{DD} = 15\text{ V}$

TYPICAL PERFORMANCE CHARACTERISTICS

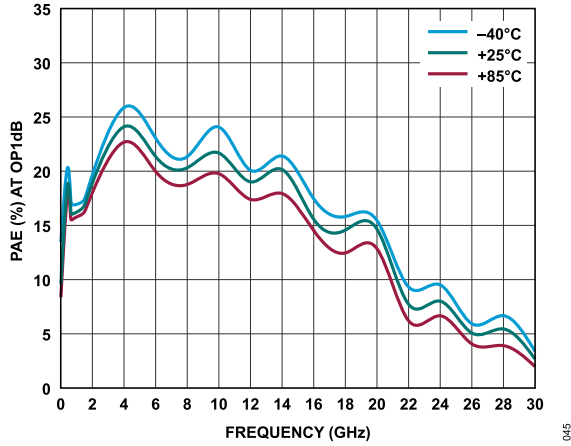


Figure 45. Power-Added Efficiency (PAE) at OP1dB vs. Frequency for Various Temperatures,  $V_{DD} = 15\text{ V}$ ,  $I_{DQ} = 500\text{ mA}$

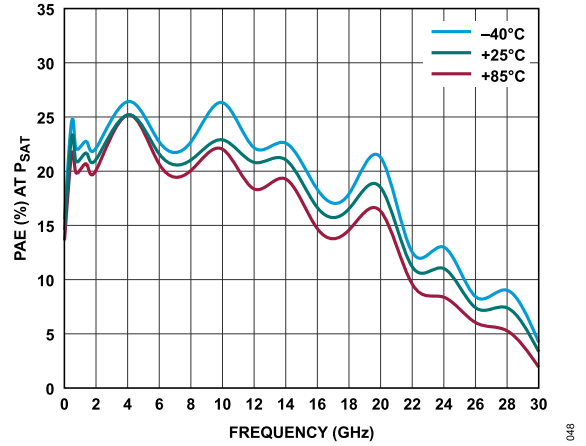


Figure 48. PAE at  $P_{SAT}$  vs. Frequency for Various Temperatures,  $V_{DD} = 15\text{ V}$ ,  $I_{DQ} = 500\text{ mA}$

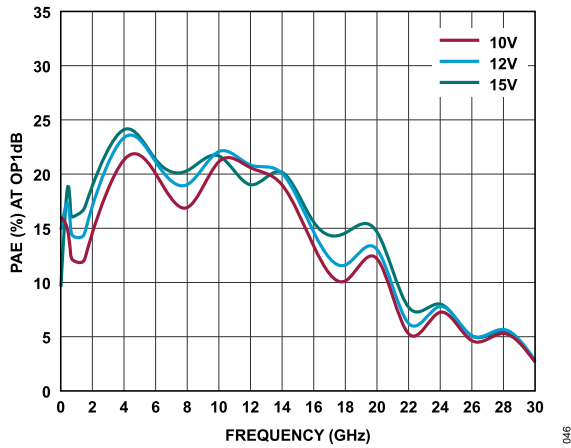


Figure 46. PAE at OP1dB vs. Frequency for Various  $V_{DD}$  Values,  $I_{DQ} = 500\text{ mA}$

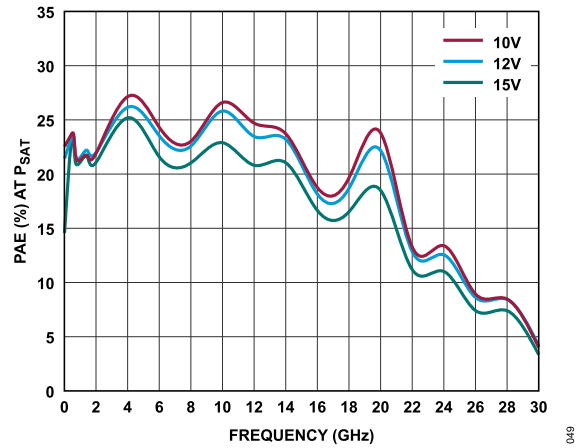


Figure 49. PAE at  $P_{SAT}$  vs. Frequency for Various  $V_{DD}$  Values,  $I_{DQ} = 500\text{ mA}$

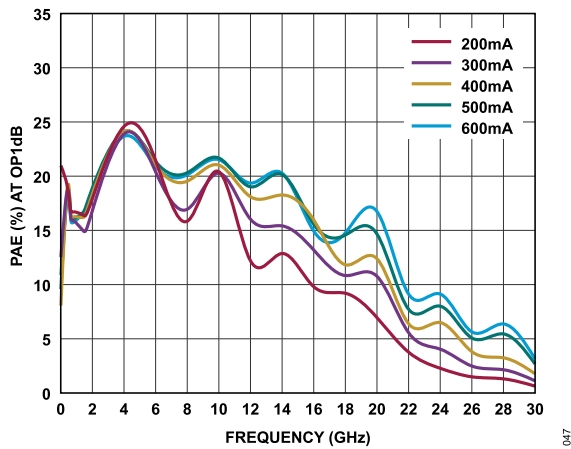


Figure 47. PAE at OP1dB vs. Frequency for Various  $I_{DQ}$  Values,  $V_{DD} = 15\text{ V}$

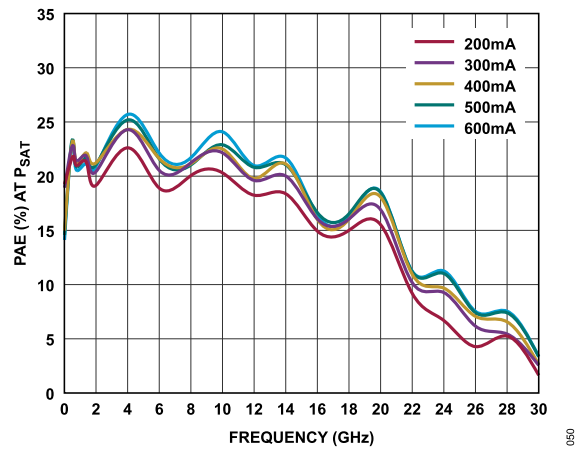


Figure 50. PAE at  $P_{SAT}$  vs. Frequency for Various  $I_{DQ}$  Values,  $V_{DD} = 15\text{ V}$

TYPICAL PERFORMANCE CHARACTERISTICS

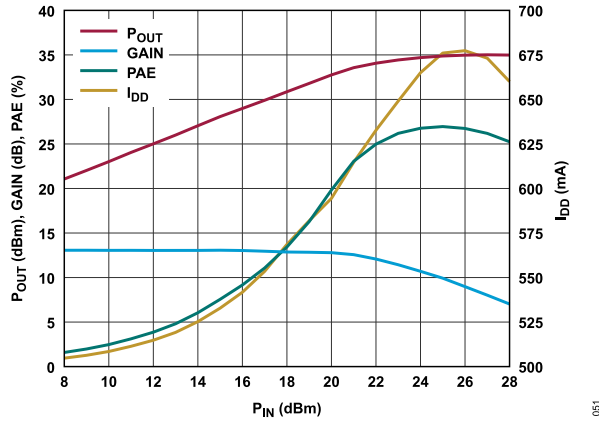


Figure 51.  $P_{OUT}$ , GAIN, PAE, and  $I_{DD}$  vs.  $P_{IN}$ , 4 GHz,  $V_{DD} = 15$  V,  $I_{DQ} = 500$  mA

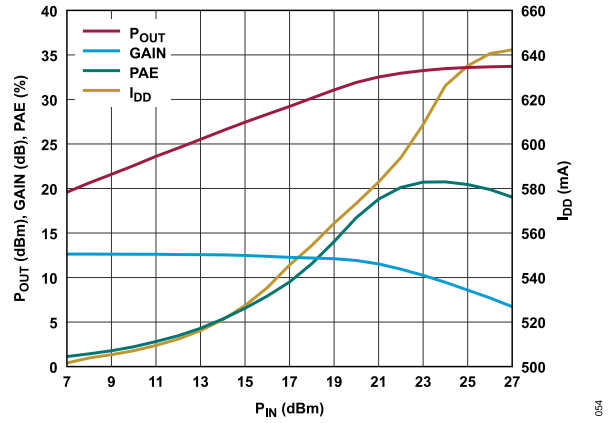


Figure 54.  $P_{OUT}$ , GAIN, PAE, and  $I_{DD}$  vs.  $P_{IN}$ , 8 GHz,  $V_{DD} = 15$  V,  $I_{DQ} = 500$  mA

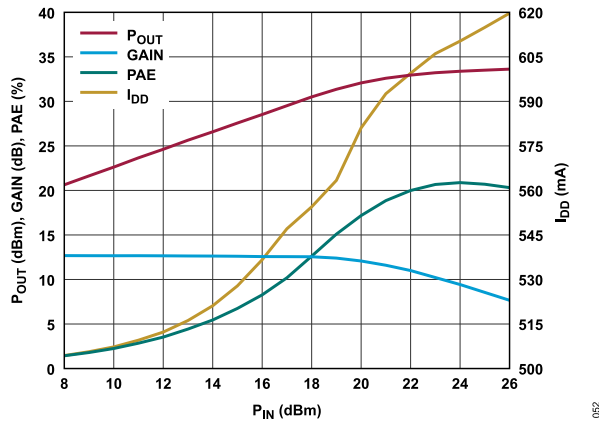


Figure 52.  $P_{OUT}$ , GAIN, PAE, and  $I_{DD}$  vs.  $P_{IN}$ , 12 GHz,  $V_{DD} = 15$  V,  $I_{DQ} = 500$  mA

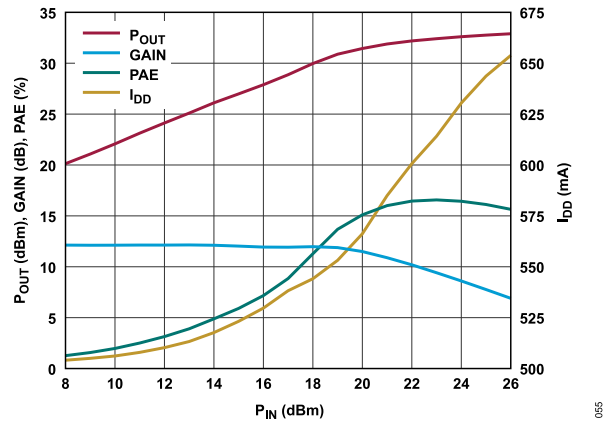


Figure 55.  $P_{OUT}$ , GAIN, PAE, and  $I_{DD}$  vs.  $P_{IN}$ , 16 GHz,  $V_{DD} = 15$  V,  $I_{DQ} = 500$  mA

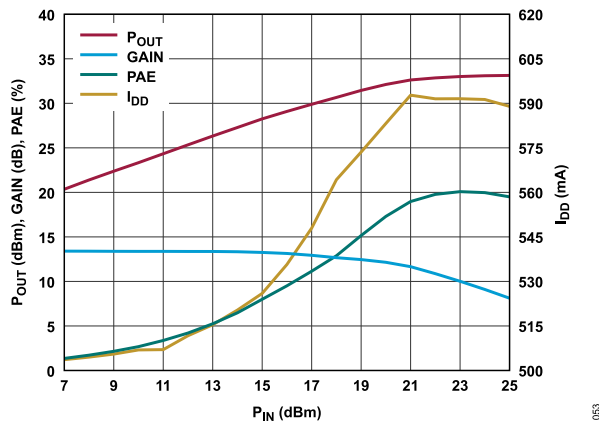


Figure 53.  $P_{OUT}$ , GAIN, PAE, and  $I_{DD}$  vs.  $P_{IN}$ , 20 GHz,  $V_{DD} = 15$  V,  $I_{DQ} = 500$  mA

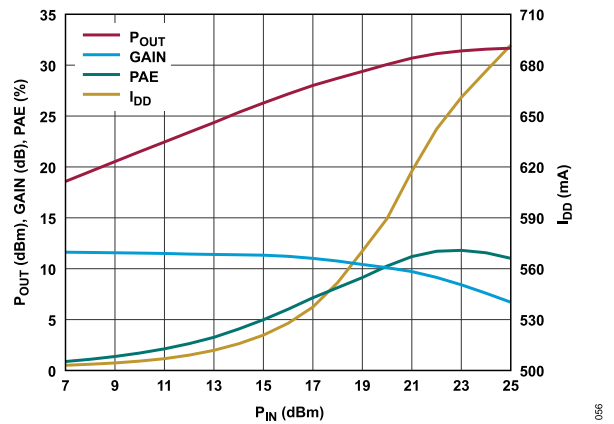


Figure 56.  $P_{OUT}$ , GAIN, PAE, and  $I_{DD}$  vs.  $P_{IN}$ , 24 GHz,  $V_{DD} = 15$  V,  $I_{DQ} = 500$  mA

TYPICAL PERFORMANCE CHARACTERISTICS

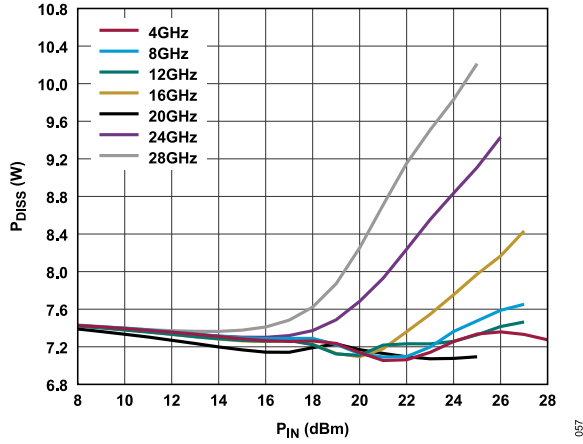


Figure 57.  $P_{DISS}$  vs.  $P_{IN}$  for Various Frequencies at  $T_A = 85^\circ\text{C}$ ,  $V_{DD} = 15\text{ V}$ ,  $I_{DQ} = 500\text{ mA}$

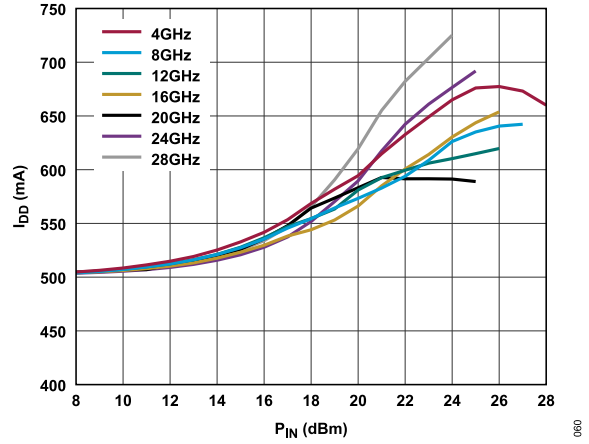


Figure 60.  $I_{DD}$  vs.  $P_{IN}$  for Various Frequencies,  $V_{DD} = 15\text{ V}$ ,  $I_{DQ} = 500\text{ mA}$

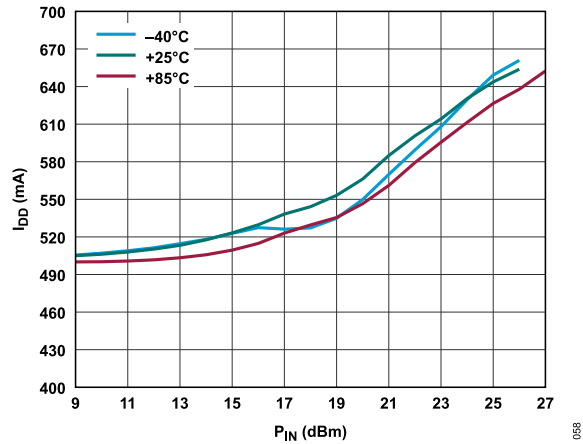


Figure 58.  $I_{DD}$  vs.  $P_{IN}$  for Various Temperatures,  $16\text{ GHz}$ ,  $V_{DD} = 15\text{ V}$ ,  $I_{DQ} = 500\text{ mA}$

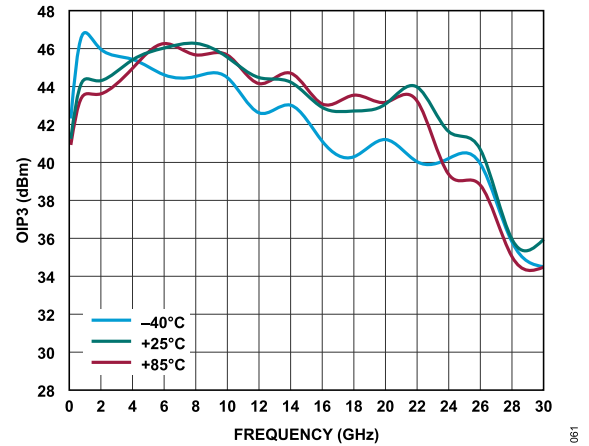


Figure 61.  $OIP3$  vs. Frequency for Various Temperatures,  $P_{OUT}$  per Tone =  $16\text{ dBm}$ ,  $V_{DD} = 15\text{ V}$ ,  $I_{DQ} = 500\text{ mA}$

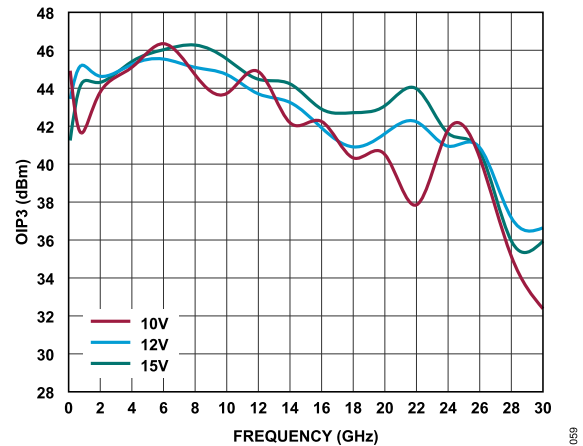


Figure 59.  $OIP3$  vs. Frequency for Various  $V_{DD}$  Values,  $P_{OUT}$  per Tone =  $16\text{ dBm}$ ,  $I_{DQ} = 500\text{ mA}$

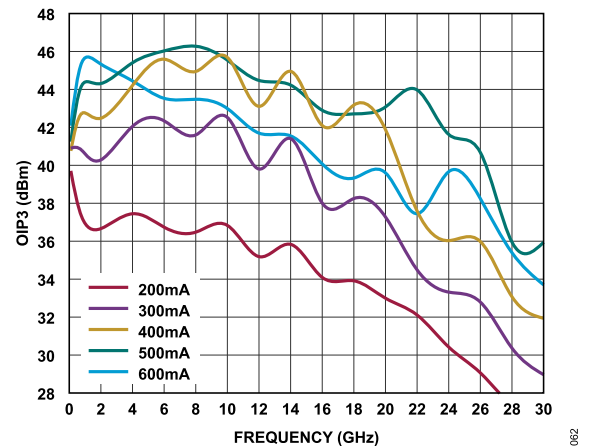


Figure 62.  $OIP3$  vs. Frequency for Various  $I_{DQ}$  Values,  $P_{OUT}$  per Tone =  $16\text{ dBm}$ ,  $V_{DD} = 15\text{ V}$

TYPICAL PERFORMANCE CHARACTERISTICS

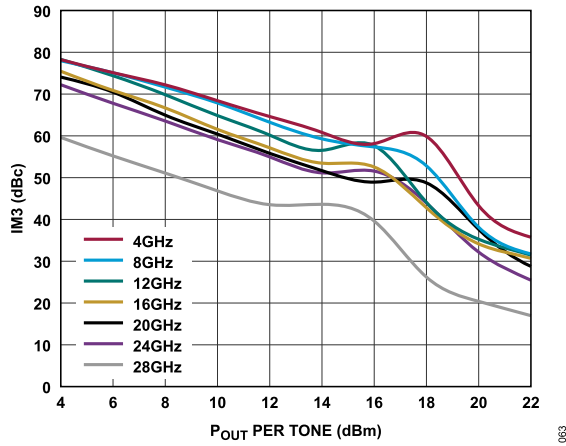


Figure 63. Third-Order Intermodulation Distortion (IM3) vs.  $P_{OUT}$  per Tone for Various Frequencies,  $V_{DD} = 10\text{ V}$ ,  $I_{DQ} = 500\text{ mA}$

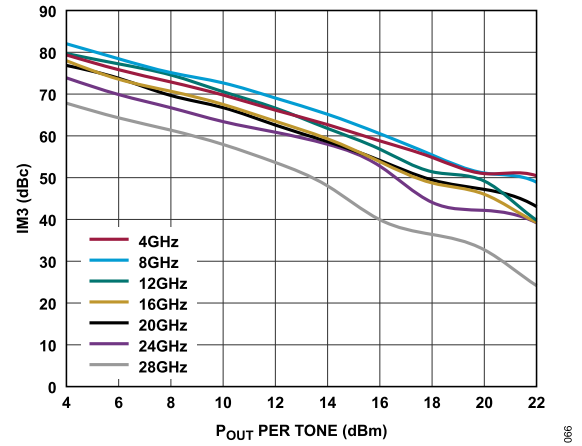


Figure 66. IM3 vs.  $P_{OUT}$  per Tone for Various Frequencies,  $V_{DD} = 15\text{ V}$ ,  $I_{DQ} = 500\text{ mA}$

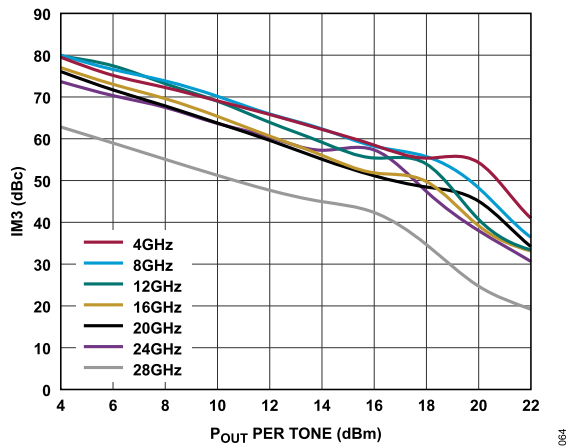


Figure 64. IM3 vs.  $P_{OUT}$  per Tone for Various Frequencies,  $V_{DD} = 12\text{ V}$ ,  $I_{DQ} = 500\text{ mA}$

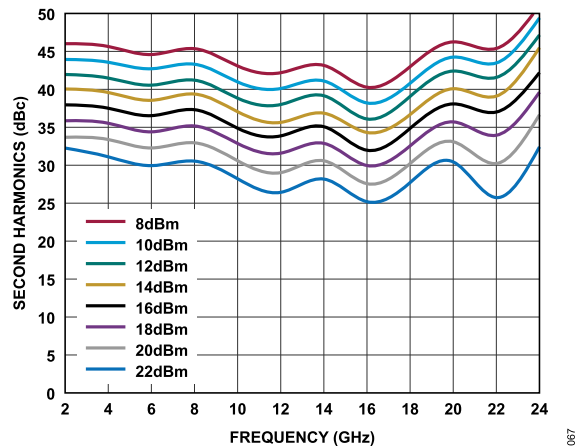


Figure 67. Second Harmonics vs. Frequency for Various  $P_{OUT}$  Values,  $V_{DD} = 15\text{ V}$ ,  $I_{DQ} = 500\text{ mA}$

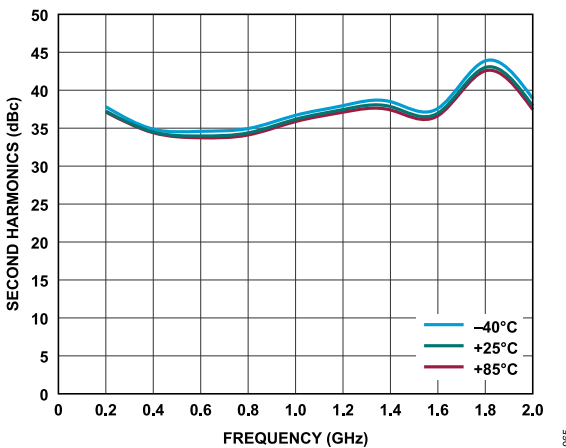


Figure 65. Low Frequency Second Harmonics vs. Frequency for Various Temperatures,  $V_{DD} = 15\text{ V}$ ,  $I_{DQ} = 500\text{ mA}$ ,  $P_{OUT} = 16\text{ dBm}$

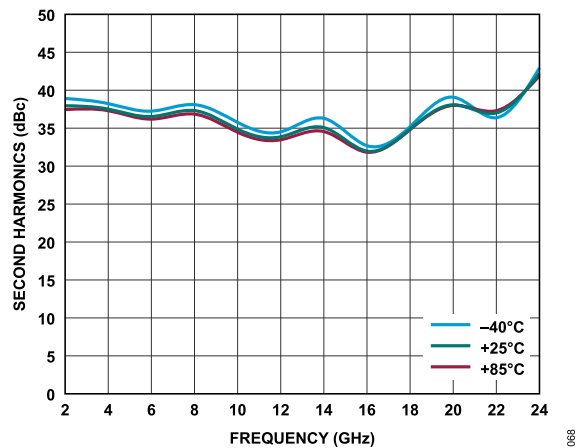


Figure 68. Second Harmonics vs. Frequency for Various Temperatures,  $V_{DD} = 15\text{ V}$ ,  $I_{DQ} = 500\text{ mA}$ ,  $P_{OUT} = 16\text{ dBm}$

TYPICAL PERFORMANCE CHARACTERISTICS

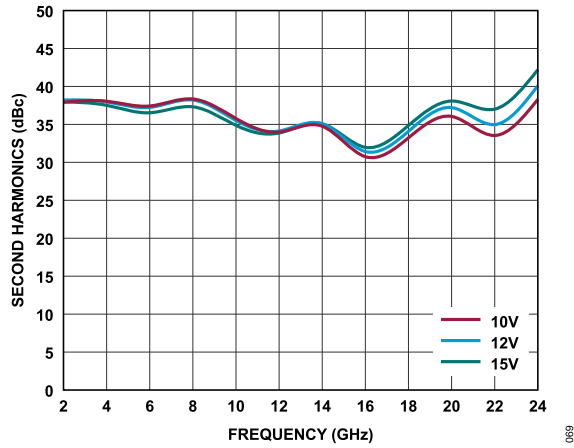


Figure 69. Second Harmonics vs. Frequency for Various  $V_{DD}$  Values,  $I_{DQ} = 500\text{ mA}$ ,  $P_{OUT} = 16\text{ dBm}$

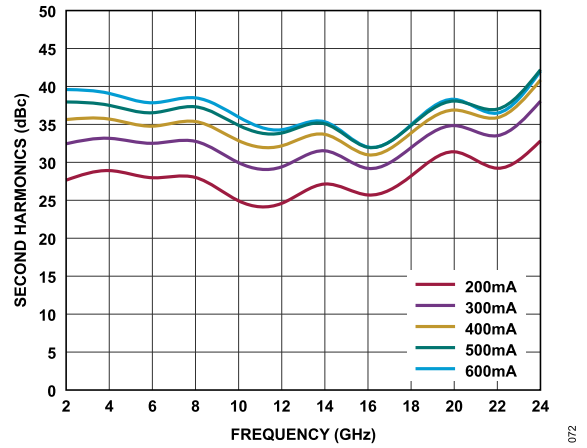


Figure 72. Second Harmonics vs. Frequency for Various  $I_{DQ}$  Values,  $V_{DD} = 15\text{ V}$ ,  $P_{OUT} = 16\text{ dBm}$

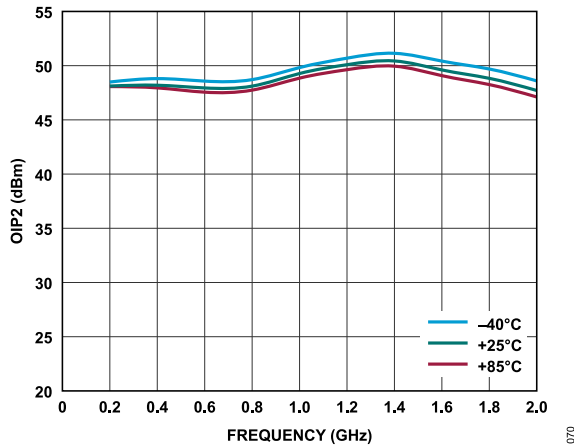


Figure 70. Low Frequency OIP2 vs. Frequency for Various Temperatures,  $V_{DD} = 15\text{ V}$ ,  $I_{DQ} = 500\text{ mA}$ ,  $P_{OUT} = 16\text{ dBm}$

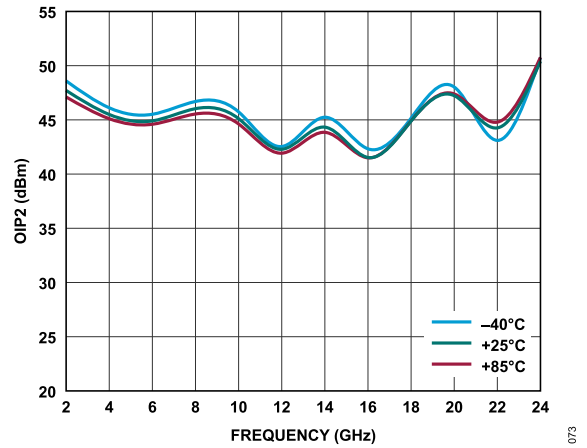


Figure 73. OIP2 vs. Frequency for Various Temperatures,  $V_{DD} = 15\text{ V}$ ,  $I_{DQ} = 500\text{ mA}$ ,  $P_{OUT} = 16\text{ dBm}$

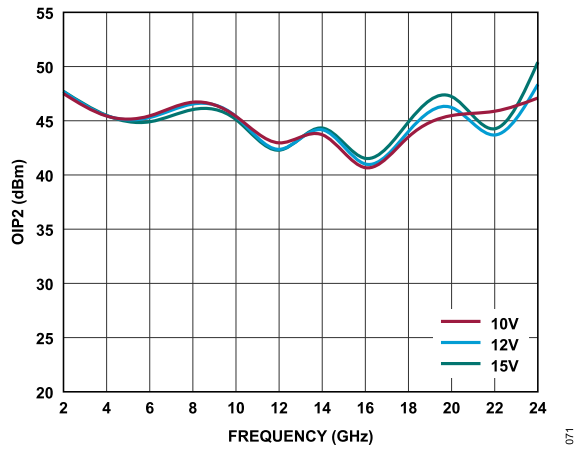


Figure 71. OIP2 vs. Frequency for Various  $V_{DD}$  Values,  $I_{DQ} = 500\text{ mA}$ ,  $P_{OUT} = 16\text{ dBm}$

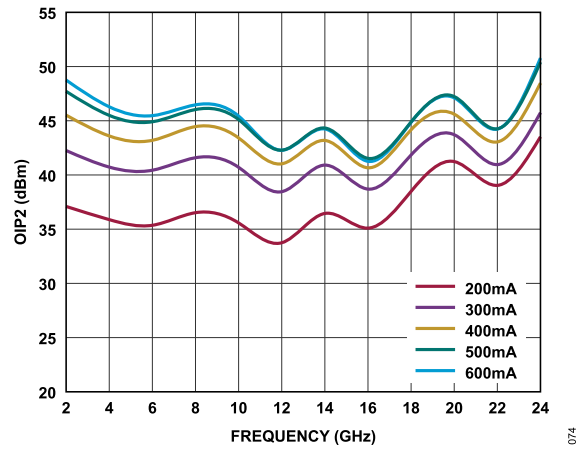


Figure 74. OIP2 vs. Frequency for Various  $I_{DQ}$  Values,  $V_{DD} = 15\text{ V}$ ,  $P_{OUT} = 16\text{ dBm}$

TYPICAL PERFORMANCE CHARACTERISTICS

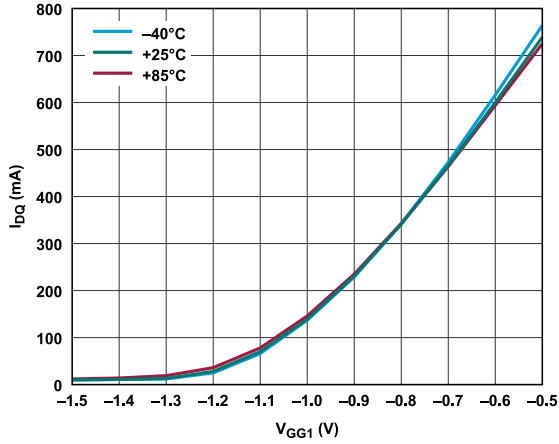


Figure 75.  $I_{DQ}$  vs.  $V_{GG1}$  for Various Temperatures,  $V_{DD} = 15\text{V}$

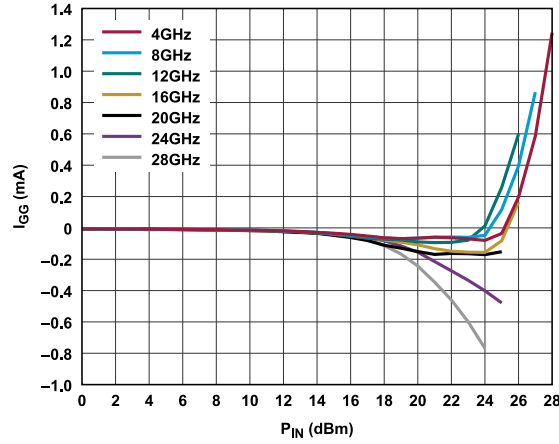


Figure 78.  $I_{GG}$  vs.  $P_{IN}$  for Various Frequencies,  $V_{DD} = 15\text{V}$

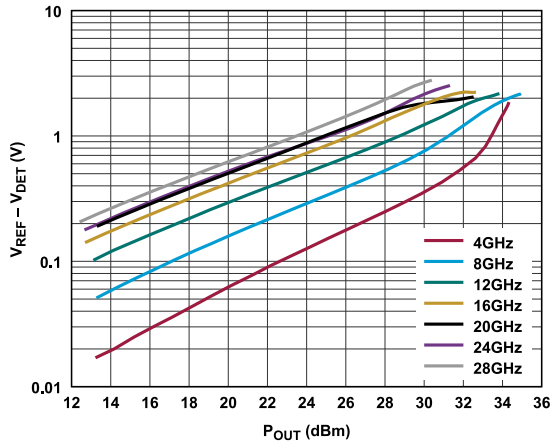


Figure 76. Detector Voltage ( $V_{REF} - V_{DET}$ ) vs.  $P_{OUT}$  for Various Frequencies

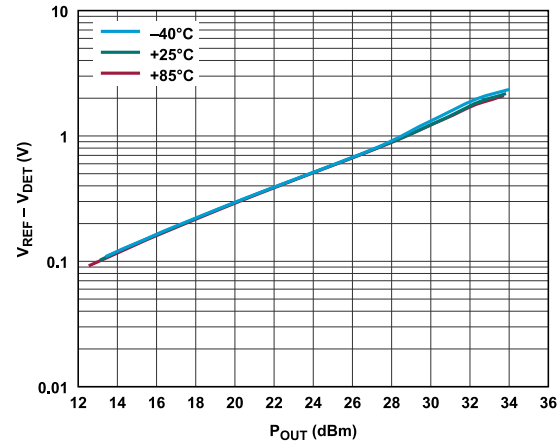


Figure 79.  $V_{REF} - V_{DET}$  vs.  $P_{OUT}$  for Various Temperatures at 12 GHz

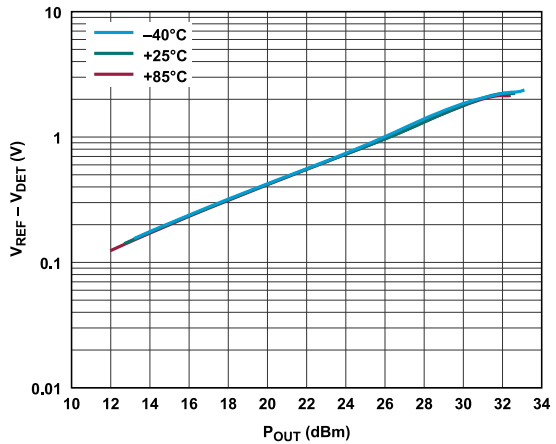


Figure 77.  $V_{REF} - V_{DET}$  vs.  $P_{OUT}$  for Various Temperatures at 16 GHz

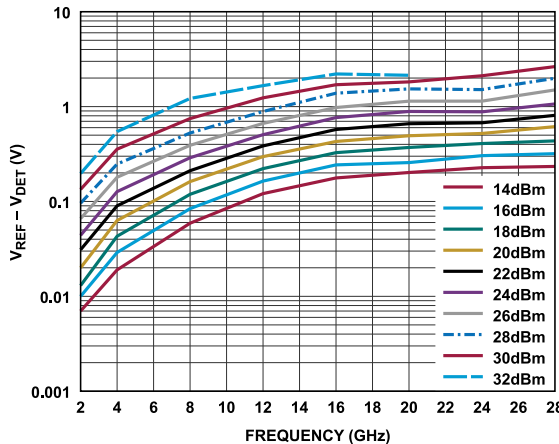


Figure 80.  $V_{REF} - V_{DET}$  vs. Frequency for Various  $P_{OUT}$  Values

TYPICAL PERFORMANCE CHARACTERISTICS

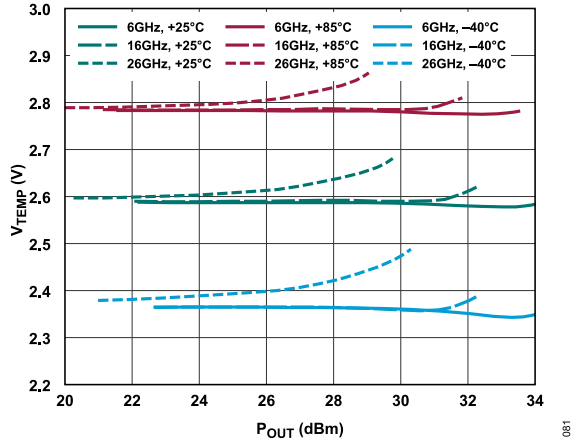


Figure 81. Temperature Sensor Voltage ( $V_{TEMP}$ ) vs.  $P_{OUT}$  for Various Frequencies and Temperatures,  $V_{DD} = 15\text{ V}$ ,  $I_{DQ} = 500\text{ mA}$

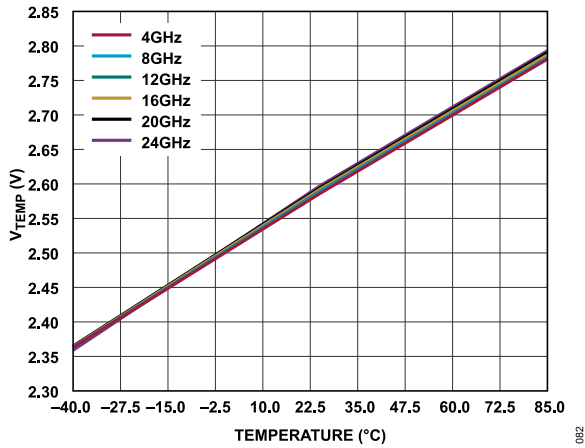


Figure 82.  $V_{TEMP}$  vs. Temperature for Various Frequencies,  $P_{OUT} = 28\text{ dBm}$ ,  $V_{DD} = 15\text{ V}$ ,  $I_{DQ} = 500\text{ mA}$

## THEORY OF OPERATION

The ADPA9007 is a broadband distributed GaAs, pHEMT, medium power amplifier. The simplified block diagram is shown in [Figure 83](#). The drain current is set by the negative voltage applied to the VGG1 pin. The gate pin, VGG1, is driven by a negative voltage in the  $-1.5\text{ V}$  to  $0\text{ V}$  range. For an  $I_{DQ}$  of  $500\text{ mA}$ , a gate bias voltage of  $-0.7\text{ V}$  is typically required. The drain bias voltage is applied through the RFOUT/VDD pin via a broadband bias tee or external bias network.

A portion of the RF output signal is directionally coupled to a diode for detection of the RF output power. When the diode is DC biased, the diode rectifies the RF power and makes the RF power available for measurement as DC voltage at the VDET pin. To allow temperature compensation of the VDET pin, an identical circuit (minus the RF coupled power) is available via the VREF pin. Taking the difference of  $V_{REF} - V_{DET}$  provides a temperature compensated signal that is proportional to the RF output power.

The ADPA9007 contains an integrated temperature sensor. The temperature sensor that is biased using the VBTEMP pin and a voltage that is proportional to the device temperature is available on VTEMP pin.

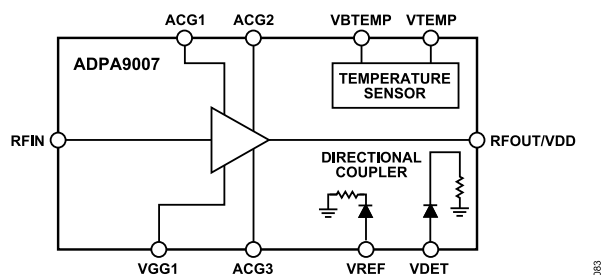


Figure 83. ADPA9007 Architecture



**BIASING THE ADPA9007 WITH THE HMC980LP4E**

The HMC980LP4E is an active bias controller that is designed to meet the bias requirements of depletion mode amplifiers such as the ADPA9007. The controller provides constant drain current biasing over temperature, device to device variation, and it properly sequences gate and drain voltages to ensure the safe operation of the amplifier. The HMC980LP4E also offers self-protection in the event of a short circuit. An internal charge pump generates the negative voltage that is needed on the gate of the ADPA9007, and there is an option to use an external negative voltage source. The HMC980LP4E is also available in die form as the HMC980-Die.

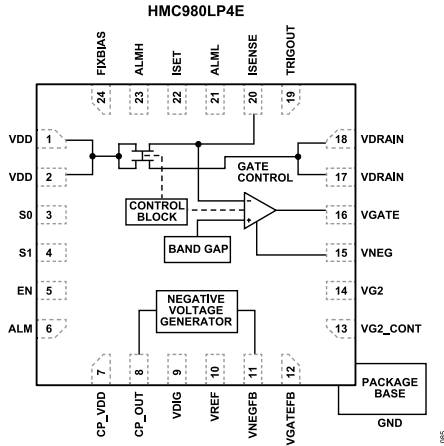


Figure 85. HMC980LP4E Active Bias Control

**APPLICATION CIRCUIT SETUP**

Figure 86 shows an application circuit using the HMC980LP4E to control the ADPA9007. When using an external negative supply for VNEG, see the application circuit shown in Figure 87.

In the application circuit shown in Figure 86, the ADPA9007 drain voltage ( $V_{DRAIN}$ ) and drain current ( $I_{DRAIN}$ ) are set by the following equations:

$$V_{DD} = V_{DRAIN} + (I_{DRAIN} \times 1.55 \Omega) \tag{1}$$

$$V_{DD} = 15 V + (0.6 A \times 1.55 \Omega) = 15.93 V \tag{2}$$

where:

The  $V_{DD}$  and  $V_{DRAIN}$  values are in volts.

The  $I_{DRAIN}$  value is in amperes.

$$R10 = (150 \Omega \times A) / (I_{DRAIN}) \tag{3}$$

$$R10 = (150 \Omega \times A) / (0.6 A) = 250 \Omega \tag{4}$$

where:

The  $R10$  is in ohms.

The  $I_{DRAIN}$  is in amperes.

To achieve a certain large signal output power, sufficient drain current must be available to the device. The required drain current can be estimated from the curves shown in Figure 51 to Figure 56. As an example, for 16 GHz at  $I_{DQ} = 500$  mA in constant gate voltage mode, Figure 55 shows that the  $I_{DD}$  ramps up to approximately 600 mA at P1dB. In order to obtain similar P1dB performance in constant drain current mode, the constant drain current must thus be set higher than 500 mA, so that 600 mA is available to the device. This can be seen in Figure 95. If the constant drain current were to instead be set to 500 mA, then 600 mA would not be available to the device at large signal, resulting in a lower P1dB.

**LIMITING VGATE FOR THE ADPA9007  $V_{GG1}$**

When using the HMC980LP4E to control the ADPA9007, the minimum gate voltage should be set to approximately  $-1.5$  V. To set the minimum voltages, set the R15 and R16 resistors to the values shown in Figure 86 and Figure 87. Refer to the AN-1363: Meeting Biasing Requirements of Externally Biased RF/Microwave Amplifiers with Active Bias Controllers application note for more information and calculations for the R15 and R16 resistors.

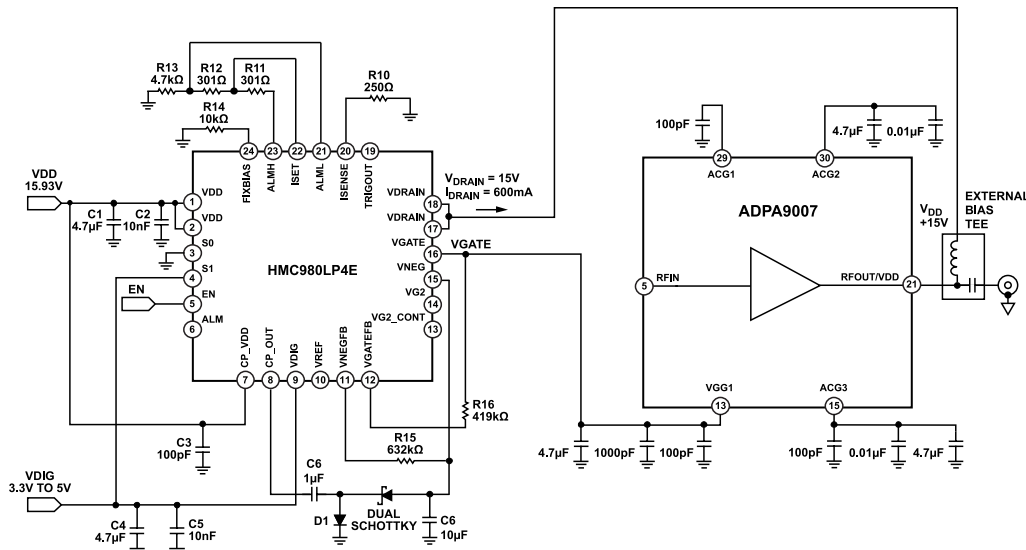


Figure 86. Application Circuit Using the HMC980LP4E with the ADPA9007 (Internal Negative Voltage Source)

## BIASING THE ADPA9007 WITH THE HMC980LP4E

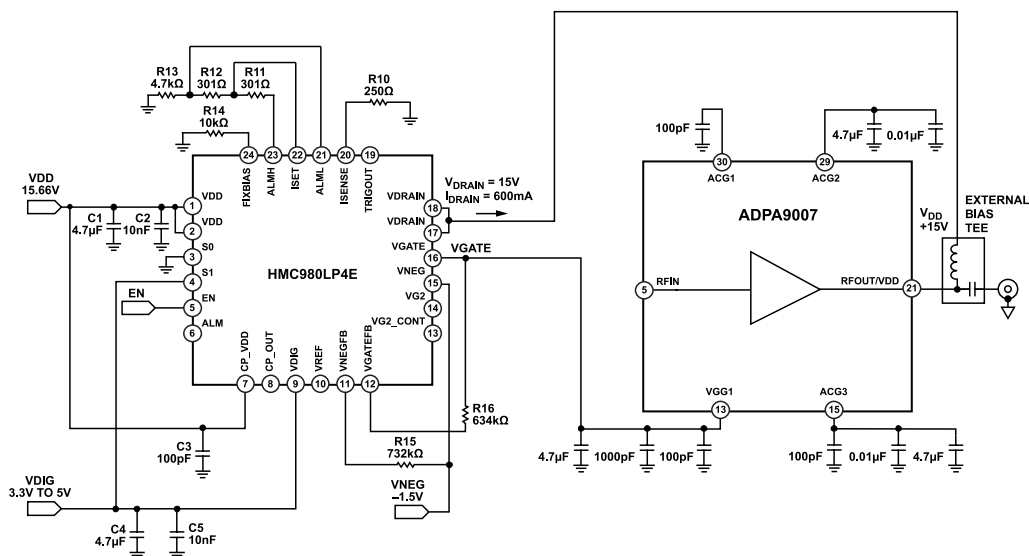


Figure 87. Application Circuit Using the HMC980LP4E with the ADPA9007 (External Negative Voltage Source)

## HMC980LP4E BIAS SEQUENCE

The DC supply sequence described in this section is required to prevent damage to the HMC980LP4E when using the device to control the ADPA9007.

### Power-Up Sequence

The power-up sequence for the HMC980LP4E is as follows:

1. Set the VDIG pin = 3.3 V.
2. Set the S0 pin = 3.3 V.
3. Set the VDD pin = 15.51 V.
4. Set the VNEG pin = -1.5 V (this step is unnecessary if using an internally generated voltage).
5. Set the EN pin = 3.3 V (the transition from 0 V to 3.3 V turns on the VGATE pin and the VDRAIN pin).

### Power-Down Sequence

The power-down sequence for the HMC980LP4E is as follows:

1. Set the EN pin = 0 V (the transition from 3.3 V to 0 V turns off the VDRAIN pins and the VGATE pin).
2. Set the VNEG pin = 0 V (this step is unnecessary if using and internally generated voltage).
3. Set the VDD pin = 0 V.
4. Set the S0 pin = 0 V.
5. Set the VDIG pin = 0 V.

After the HMC980LP4E bias control circuit is set up, toggle the bias to the ADPA9007 on or off by applying 3.3 V or 0 V, respectively, to the EN pin. At the EN pin = +3.3 V, the VGATE pin drops to -1.5 V, and the VDRAIN pins turn on at +15 V. The VGATE pin then rises until  $I_{DRAIN} = 600$  mA, and the closed control loop regulates

$I_{DRAIN}$  at 600 mA. When the EN pin = 0 V, the VGATE pin is set to -1.5 V, and the VDRAIN pins are set to 0 V.

## CONSTANT DRAIN CURRENT BIASING VS. CONSTANT GATE VOLTAGE BIASING

The HMC980LP4E uses closed-loop feedback to continuously adjust the VGATE pin to maintain a constant drain current bias over DC supply variation, temperature, and device-to-device variation. In addition, constant drain current biasing is the optimum method to reduce time in calibration procedures and to maintain consistent performance over time.

To increase the OP1dB performance for the constant drain current bias, increase the set-point current as shown in Figure 89. The limit of increasing set-point current under the constant drain current operation is set by the thermal limitations found in Table 6 with the maximum power-dissipation specification. As the  $I_{DD}$  increases, the power dissipation increases, but the actual OP1dB does not continue to increase indefinitely. Therefore, when using constant drain current biasing, take the relationship between the power dissipation and the OP1dB performance into consideration.

BIASING THE ADPA9007 WITH THE HMC980LP4E

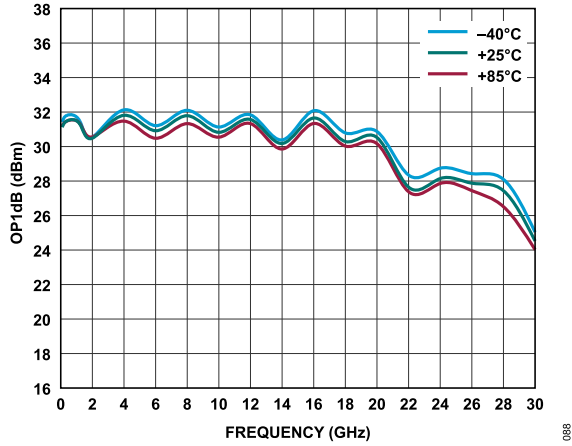


Figure 88. OP1dB vs. Frequency for Various Temperatures,  $V_{DD} = 15\text{ V}$ , Data Measured with Constant  $I_{DD} = 600\text{ mA}$

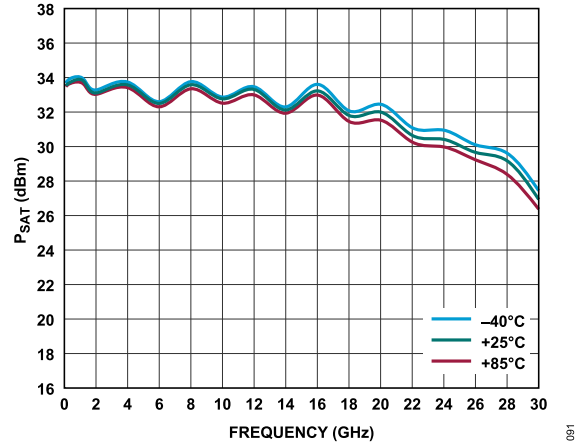


Figure 91.  $P_{SAT}$  vs. Frequency for Various Temperatures,  $V_{DD} = 15\text{ V}$ , Data Measured with Constant  $I_{DD} = 600\text{ mA}$

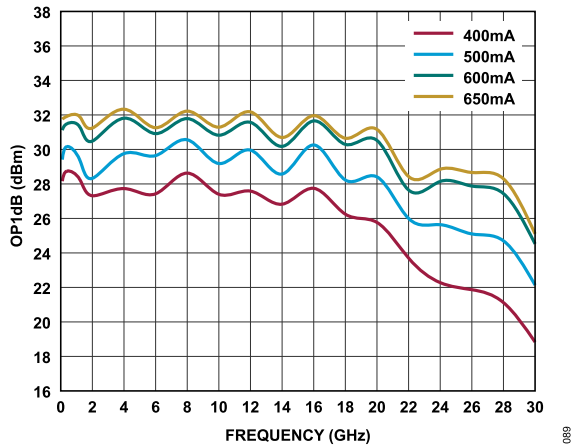


Figure 89. OP1dB vs. Frequency for Various Set-Point Drain Currents, Constant Current Mode,  $V_{DD} = 15\text{ V}$

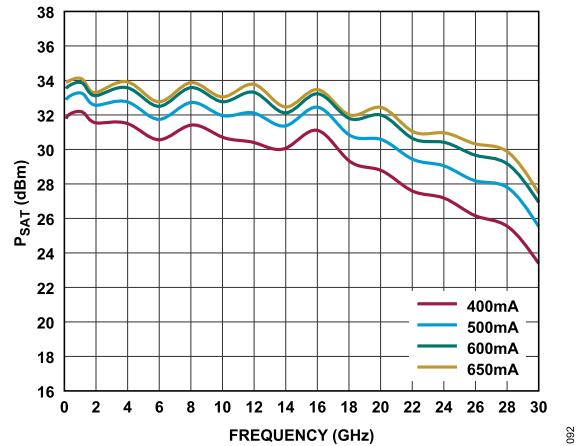


Figure 92.  $P_{SAT}$  vs. Frequency for Various Set-Point Drain Currents, Constant Current Mode,  $V_{DD} = 15\text{ V}$

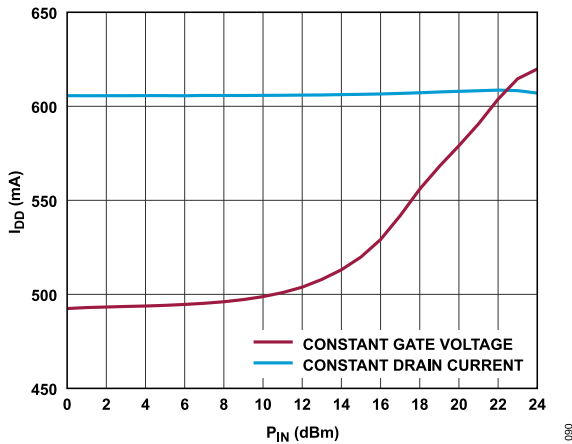


Figure 90.  $I_{DD}$  vs.  $P_{IN}$ ,  $V_{DD} = 15\text{ V}$ , Frequency = 16 GHz, Constant  $I_{DRAIN}$  Set Point = 600 mA and Constant  $V_{GG1}$  ( $I_{DQ} = 500\text{ mA}$ )

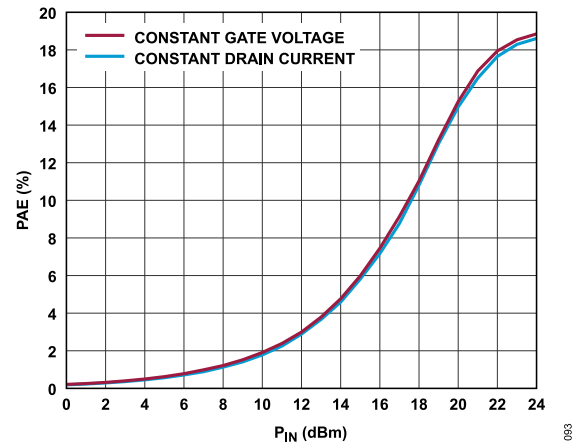


Figure 93. PAE vs.  $P_{IN}$ ,  $V_{DD} = 15\text{ V}$ , Frequency = 16 GHz, Constant  $I_{DRAIN}$  Set Point = 600 mA and Constant  $V_{GG1}$  ( $I_{DQ} = 500\text{ mA}$ )

BIASING THE ADPA9007 WITH THE HMC980LP4E

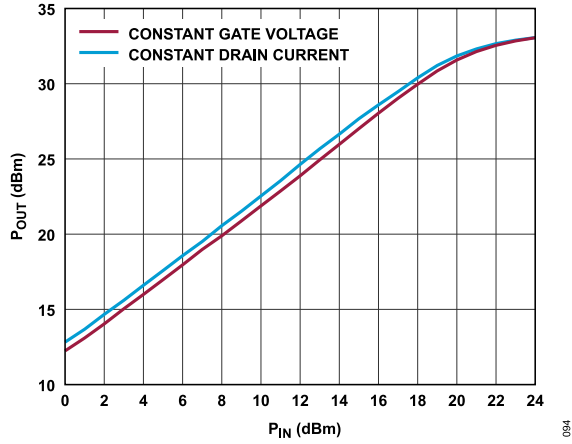


Figure 94. P<sub>OUT</sub> vs. P<sub>IN</sub>, V<sub>DD</sub> = 15 V, Frequency = 16 GHz, Constant I<sub>DRAIN</sub> Set Point = 600 mA and Constant V<sub>GG1</sub> (I<sub>DQ</sub> = 500 mA)

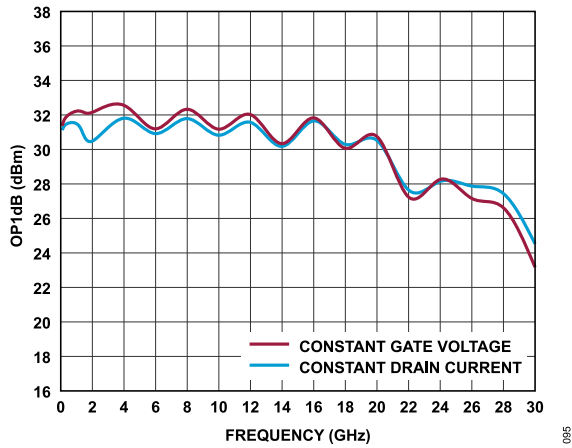


Figure 95. OP1dB vs. Frequency, V<sub>DD</sub> = 15 V, Constant I<sub>DRAIN</sub> Set Point = 600 mA and Constant V<sub>GG1</sub> (I<sub>DQ</sub> = 500 mA)

OUTLINE DIMENSIONS

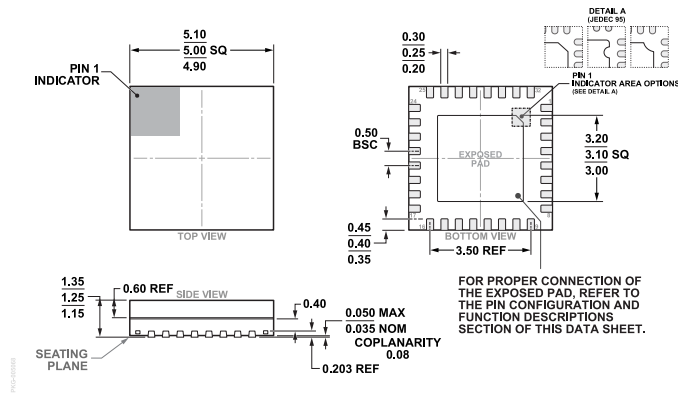


Figure 96. 32-Lead Lead Frame Chip Scale Package, Premolded Cavity [LFCSP\_CAV] 5 mm × 5 mm Body and 1.25 mm Package Height (CG-32-2) Dimensions shown in millimeters

Updated: August 11, 2023

ORDERING GUIDE

Model <sup>1</sup>	Temperature Range	Package Description	Packing Quantity	Package Option
ADPA9007ACGZN	-40°C to +85°C	32-Lead LFCSP (5 mm × 5 mm w/ EP)	Reel, 100	CG-32-2
ADPA9007ACGZN-R7	-40°C to +85°C	32-Lead LFCSP (5 mm × 5 mm w/ EP)	Reel, 1000	CG-32-2

<sup>1</sup> Z = RoHS Compliant Part.

EVALUATION BOARDS

Model <sup>1</sup>	Description
ADPA9007-EVALZ	Evaluation Board

<sup>1</sup> Z = RoHS Compliant Part.

# Mouser Electronics

Authorized Distributor

Click to View Pricing, Inventory, Delivery & Lifecycle Information:

[Analog Devices Inc.:](#)

[ADPA9007ACGZN-R7](#) [ADPA9007ACGZN](#)